Bifurcation of elastic curves with modulated stiffness

Katharina Brazda, Gaspard Jankowiak, Christian Schmeiser, Ulisse Stefanelli

Bifurcation of elastic curves with modulated stiffness

Katharina Brazda[1], Gaspard Jankowiak[2], Christian Schmeiser[1], Ulisse Stefanelli[1,3,4]

[1]University of Vienna, Faculty of Mathematics, Oskar-Morgenstern-Platz 1, 1090 Wien, Austria

[2]Radon Institute for Applied and Computational Mathematics, Altenbergerstr. 69, 4040, Linz, Austria

[3]Vienna Research Platform on Accelerating Photoreaction Discovery, University of Vienna, Währingerstraße 17, 1090 Wien, Austria

[4]Istituto di Matematica Applicata e Tecnologie Informatiche *E. Magenes*, via Ferrata 1, I-27100 Pavia, Italy

November 26, 2020

Abstract

We investigate the equilibrium configurations of closed planar elastic curves of fixed length, whose stiffness (bending rigidity) depends on an additional density variable. The underlying variational model relies on the minimization of a bending energy with respect to shape and density and can be considered as a one-dimensional analogue of the Canham-Helfrich model for heterogeneous biological membranes. We present a generalized Euler-Bernoulli elastica functional featuring a density-dependent stiffness coefficient. In order to treat the inherent nonconvexity of the problem we introduce an additional regularization term. Then, we derive the system of Euler-Lagrange equations and study the bifurcation structure of solutions with respect to the model parameters. We present analytical results and numerical simulations.

Contents

1 Introduction

We are interested in the configurations of elastic curves featuring an additional scalar density variable that changes the stiffness. This study is motivated by the variational model for the *shapes of biological membranes*, originally proposed by Canham [5] and Helfrich [10] to explain the characteristic biconcave shape of a human red blood cell. According to this model, the equilibrium membrane shape Σ minimizes the bending energy

$$E_{\mathrm{CH}}(\Sigma) = \int_\Sigma \left(\frac{\beta}{2} (H - H_0)^2 + \gamma K \right) \mathrm{d}S$$

under suitable constraints on membrane area and enclosed volume. Here, Σ is a smooth closed surface embedded in $\mathbb{R}^3$, H is the mean curvature of Σ, K is the Gauss curvature of Σ, and the material parameters comprise the stiffnesses (bending rigidities) $\beta > 0$, $\gamma < 0$ as well as the spontaneous curvature $H_0 \in \mathbb{R}$. The material parameters of heterogeneous biomembranes will depend on the variable membrane composition, which is described by a scalar density $\rho \colon \Sigma \to \mathbb{R}$ of fixed total mass. Yet, the composition of heterogeneous membranes influences their shapes in an additional way. In fact, biomembranes mechanically behave as two-dimensional viscous incompressible fluids and the membrane constituents will freely rearrange themselves to better match the membrane geometry. Due to this *coupling effect between curvature and composition*, the energy for heterogeneous biomembranes has to be minimized with respect to both membrane geometry Σ and composition ρ. Configurations featuring this coupling have been experimentally observed for example by Baumgart, Hess, & Webb [2] in case of giant unilamellar vesicles. Furthermore, the coupling effect also plays an essential role the dynamic morphology changes of cells, where special curved membrane proteins are involved, cf. McMahon & Gallop [15].

Results on the mathematical analysis of the variational problem for heterogeneous biomembranes have been obtained for membranes whose material parameters take constant values within multiple sharply separated domains, the so-called phases. In this case, the membrane energy possesses an additional line-tension contribution at phase interfaces. Choksi, Morandotti, & Veneroni [6] and also Helmers [12] established existence of multiphase minimizers in the axisymmetric regime. Without symmetry restriction, existence of multiphase minimizers in the geometric measure theory setting of varifolds has recently been obtained by [4]. To the best of our knowledge, proving existence of minimizers for membranes featuring continuous phase densities and general material parameter models is an open problem. Here, we address this issue in the one-dimensional setting of elastic curves.

A classical elastic curve in the plane, $\gamma \colon [0, L] \to \mathbb{R}^2$, minimizes the Euler-Bernoulli elastic bending energy

$$E(\gamma) = \frac{1}{2} \int_\gamma \kappa^2 \, \mathrm{d}l,$$

where κ is the scalar curvature of γ. The stationary points are called *elastica* and can be analytically described in terms of elliptic functions. As was already clear to Euler, the only closed elastica of fixed length in the plane are the circle and Bernoulli's Figure-8 curve, the single covered circle being the unique global minimizer of E, see for example Truesdell [17] and Langer & Singer [13].

Inspired by the variational model for heterogeneous biological membranes, we are interested in the effects caused by an additional scalar density ρ that modulates the elastic behavior of the curve. For this purpose we consider the following elastic bending energy with *density-modulated stiffness*,

$$E_0(\rho, \gamma) = \frac{1}{2} \int_\gamma \beta(\rho) \, \kappa^2 \mathrm{d}l.$$

Our interest lies on the effects of the variable stiffness β. Therefore, we do not consider a one-dimensional counterpart for the spontaneous curvature H_0. In order to take into account the coupling between shape and composition, we have to minimize E_0 with respect to both, γ and ρ. Admissible curves γ are planar, regular, C^1-closed, and have fixed length L; admissible densities ρ have fixed mass $\int_\gamma \rho \, \mathrm{d}l = M$.

The application of the Direct Method for the minimization of E_0 calls for weak lower semicontinuity, which in turn requires convexity of the integrand of E_0. Yet, if convexity holds, only the trivial minimizer exists, namely the constant density $\rho_0 = M/L$ on a circle with curvature $\kappa_0 = 2\pi/L$. This however does not correspond to the rich geometric morphologies that can be found in biological membranes. Therefore, we relax the convexity constraint and of the integrand of E_0 and consider the following regularized energy E_μ:

$$E_\mu(\rho, \gamma) = \frac{1}{2} \int_\gamma \left(\beta(\rho) \, \kappa^2 + \mu \, \dot{\rho}^2 \right) \mathrm{d}l, \tag{1.1}$$

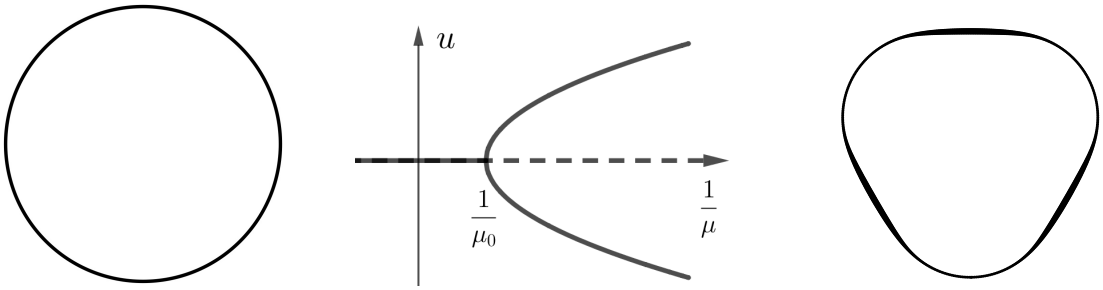

Figure 1.1: Illustration of the expected bifurcation behavior of a minimizer of E_μ (1.1). In the diagram, u represents the deviation from the trivial solution given by a circle with constant density (left). As μ decreases and $1/\mu$ passes through $1/\mu_0$, the solution is expected to develop nontrivial branches (with flip symmetry around the trivial axis). The associated nontrivial solutions (right; cf. Figure 5.4) are expected to be similar to cross-sections of heterogeneous biological membrane configurations, which are observed experimentally (e.g. Baumgart, Hess, & Webb [2]).

where μ plays the role of a regularization parameter, which physically may be interpreted as the diffusivity of the density, cf. (2.5). The existence of minimizers for E_μ is only guaranteed for $\mu > 0$, see Section 3 below. The main result of this paper is the bifurcation analysis from the trivial solution in terms of μ. We rigorously classify the bifurcation behavior of minima of E_μ. Moreover, we provide an exhaustive suite of numerical experiments, illustrating the distinguished patterning of minimizers of E_μ, depending on μ (see Figure 1.1).

A variational model for planar elastic curves with density has also been studied by Helmers [11]. He focused on the effect of spontaneous curvature and established a Γ-convergence result to the sharp interface limit. Let us mention also the recent work by Palmer & Pámpano [16], who presented analysis and numerics for the shapes of elastic rods with anisotropic bending energies.

We conclude this introduction by an outline of the paper. In Section 2 we briefly describe the mathematical setting and explain our notation. Section 3 is devoted to the justification of our model by existence and nonexistence results for minimizers. In Section 4 we analytically discuss the local bifurcation structure of solutions to the associated Euler-Lagrange equations. Numerical results for the bifurcation branches as well as for the configurations of the curves are presented in Section 5.

2 Mathematical setting

We devote this section to make the mathematical setting precise. In particular, we fix notation and comment on the existence and nonexistence issues that have been mentioned in the Introduction.

2.1 Notation and preliminaries on curves

We collect some basic information on curves [9]. In the following, we will consider *planar curves* $\gamma = (x, y) \in H^2(0, L)^2 \subset C^1([0, L])^2$, which we systematically assume to be parametrized by arc-length, namely, $|\dot\gamma| = 1$. This induces that $\ddot\gamma \in L^2(0, L)^2$ is orthogonal to $\dot\gamma$. The normal vector n to the curve is defined pointwise by counterclockwise rotating $\dot\gamma$ by $\pi/2$, namely, $n = \dot\gamma^\perp := (-\dot y, \dot x)$. The rate of change of $\dot\gamma$ in direction n is measured by the scalar *curvature* $\kappa = n \cdot \ddot\gamma \in L^2(0, L)$ of the curve, so that $\ddot\gamma = (n \cdot \ddot\gamma)\, n = \kappa\, n$.

The *inclination angle* $\theta \in H^1(0, L)$ is the angle between the tangent $\dot\gamma$ and the horizontal axis, namely, $\dot\gamma = (\dot x, \dot y) = (\cos\theta, \sin\theta)$. The curvature function $\kappa \in L^2(0, L)$ uniquely determines the curve $\gamma \in H^2(0, L)^2$ up to translations and rotations in $\mathbb{R}^2$ [9, Section 1-5, pp. 19, 24, and Section 1-7, p. 36]. In particular, if $|\dot\gamma| = 1$, then

$$\kappa = \dot\theta, \qquad \theta(s') = \theta(0) + \int_0^{s'} \kappa(s'')\,\mathrm{d}s'', \quad \text{and} \quad \gamma(s) = \begin{pmatrix} x(s) \\ y(s) \end{pmatrix} = \begin{pmatrix} x(0) \\ y(0) \end{pmatrix} + \int_0^s \begin{pmatrix} \cos\theta(s') \\ \sin\theta(s') \end{pmatrix} \mathrm{d}s'. \tag{2.1}$$

Identifying all curves whose images only differ by isometries in $\mathbb{R}^2$, one may adapt the coordinate system to $x(0) = y(0) = \theta(0) = 0$, corresponding indeed to the choice $\gamma(0) = (0, 0)$ and $\dot\gamma(0) = (1, 0)$.

A curve $\gamma\colon [0, L] \to \mathbb{R}^2$ is said to be *C^k-closed* ($k \in \mathbb{N}_0$) if γ is C^k and $\gamma^{(l)}(0) = \gamma^{(l)}(L)$ for all $0 \le l \le k$ (simply

closed for $k=0$). In particular, a curve $\gamma \in H^2(0,L)^2$ parametrized by arc-length is C^1-closed if and only if

$$0 = \gamma(L) - \gamma(0) = \int_0^L \dot\gamma(s)\mathrm{d}s = \int_0^L \begin{pmatrix}\cos\theta(s)\\ \sin\theta(s)\end{pmatrix}\mathrm{d}s = \int_0^L \begin{pmatrix}\cos\left(\theta(0)+\int_0^s \kappa(t)\,\mathrm{d}t\right)\\ \sin\left(\theta(0)+\int_0^s \kappa(t)\,\mathrm{d}t\right)\end{pmatrix}\mathrm{d}s \quad \text{and}$$
$$0 = \dot\gamma(L) - \dot\gamma(0) = (\cos\theta(L) - \cos\theta(0), \sin\theta(L) - \sin\theta(0)).$$

The latter is equivalent to $\theta(L)-\theta(0) = \int_0^L \kappa(s)\,\mathrm{d}s = 2\pi I$ for $I \in \mathbb{Z}$, where the *rotation index* $I \in \mathbb{Z}$ measures the complete turns of the tangent vector $\dot\gamma$. A curve $\gamma\colon [0,L] \to \mathbb{R}^2$ is called *simple* if it is an injective map and *regular*, if it is C^1 and $\dot\gamma(t) \neq 0$ for all $t \in [0,L]$. By the Theorem of Turning Tangents [9, Section 5-6, Theorem 2, p. 396], a simple C^1-closed regular planar positively oriented C^1 curve $\gamma\colon [0,L] \to \mathbb{R}^2$ has rotation index $I=1$, that is, $\int_0^L \kappa(s)\,\mathrm{d}s = 2\pi$. This allows us to represent a simple C^1-closed curve $\gamma \in H^2(0,L)^2$ parametrized by arc-length by its inclination angle $\theta \in H^1(0,L)$ satisfying

$$\theta(0) = 0, \quad \theta(L) = 2\pi \quad \text{and} \quad \int_0^L \begin{pmatrix}\cos\theta(s)\\ \sin\theta(s)\end{pmatrix}\mathrm{d}s = 0,$$

or by its curvature $\kappa \in L^2(0,L)$, additionally satisfying

$$\int_0^L \kappa(s)\,\mathrm{d}s = 2\pi \quad \text{and} \quad \int_0^L \begin{pmatrix}\cos\left(\theta(0)+\int_0^s \kappa(t)\,\mathrm{d}t\right)\\ \sin\left(\theta(0)+\int_0^s \kappa(t)\,\mathrm{d}t\right)\end{pmatrix}\mathrm{d}s = 0.$$

Eventually, note that by requiring a planar curve to be closed restricts the possible curvature functions $\kappa\colon [0,L] \to \mathbb{R}$. According to the Four Vertex Theorem [9, Section 1-7, Theorem 2, p. 37], a smooth simple closed regular planar curve has either constant curvature (i.e. is a circle) or the curvature function possesses at least four vertices, i.e. two local minima and two local maxima. The converse statement is given in [8]: every continuous function which either is a nonzero constant or has at least four vertices is the curvature of a simple closed regular planar curve.

2.2 Elastic energies with modulated stiffness

We consider planar *curves* $\gamma \in H^2(0,L)^2$ parametrized by arc-length. With no loss of generality, we will assume from now on the length of the curve to be 2π. The scalar *density* field $\rho : (0,2\pi) \to \mathbb{R}$ is considered to be a function of the arc-length of the curve. Moreover, we are given a density-modulated stiffness with

$$\beta \in C^2(\mathbb{R}) \quad \text{with} \quad \inf\beta = \beta_m > 0. \tag{2.2}$$

In the following, we will assume (2.2) to hold throughout, without explicit mention. Note however that some results in this section are valid under weaker conditions on β as well.

Admissible curves are defined as element of the set

$$\mathscr{A} := \left\{\gamma \in H^2(0,2\pi)^2 :\ |\dot\gamma| = 1,\ \gamma(0) = \gamma(2\pi) = 0,\ \dot\gamma(0) = \dot\gamma(2\pi) = (1,0),\ \int_0^{2\pi} \det(\dot\gamma(s), \ddot\gamma(s))\,\mathrm{d}s = 2\pi\right\}.$$

In particular, admissible curves are planar, arc-length parametrized, and C^1-closed. Note that we are not enforcing injectivity of γ (i.e. γ being simple) and we just require the weaker condition $I=1$. This simplifies our tractation, having no effect on the bifurcation result.

By the representation theorem for plane curves, any admissible curve $\gamma \in \mathscr{A}$ can be recovered from its inclination angle θ or its curvature κ. Correspondingly, we can equivalently indicate admissible curves as

$$\mathscr{A} = \left\{\theta \in H^1(0,2\pi) : \int_0^{2\pi} \begin{pmatrix}\cos\theta(s)\\ \sin\theta(s)\end{pmatrix}\mathrm{d}s = \begin{pmatrix}0\\0\end{pmatrix},\ \theta(0) = 0,\ \theta(2\pi) = 2\pi\right\} \tag{2.3}$$

or

$$\mathscr{A} = \left\{\kappa \in L^2(0,2\pi) :\ \int_0^{2\pi} \begin{pmatrix}\cos\left(\int_0^s \kappa(t)\mathrm{d}t\right)\\ \sin\left(\int_0^s \kappa(t)\mathrm{d}t\right)\end{pmatrix}\mathrm{d}s = \begin{pmatrix}0\\0\end{pmatrix},\ \int_0^{2\pi} \kappa\,\mathrm{d}s = 2\pi\right\}.$$

The abuse of notation in defining the set $\mathscr{A}$ is motivated by the above-mentioned equivalence of the representations via γ, θ, and κ, up to fixing $\gamma(0)=0$ and $\dot\gamma(0)=(1,0)$ or $\theta(0)=0$.

Admissible densities ρ are asked to have fixed total mass. By possibly redefining β, one may assume such mass to be 2π, which simplifies notation. Given the parameter $\mu \in [0,\infty)$, we define

$$\mathscr{P} := \left\{\rho \in L^1(0,2\pi) :\ \mu\rho \in H^1(0,2\pi),\ \int_0^{2\pi} \rho(s)\,\mathrm{d}s = 2\pi\right\}. \tag{2.4}$$

For the sake of simplicity, we do not restrict the values of ρ to be nonnegative, which would however be sensible, for ρ is interpreted as a density. Note however that this simplification has no effect on the bifurcation results, which are actually addressing a neighborhood of the trivial state only, where ρ is constant and positive.

The *elastic energy with modulated stiffness* is defined as

$$E_\mu(\rho,\gamma) := \int_0^{2\pi} \left(\frac{1}{2}\beta(\rho)\ddot{\gamma}^2 + \frac{\mu}{2}\dot{\rho}^2\right) \mathrm{d}s. \tag{2.5}$$

Note that the energy E_μ can be equivalently rewritten as $E_\mu(\rho,\gamma) = E_\mu(\rho,\theta) = E_\mu(\rho,\kappa)$, again by abusing notation.

We identify elastic curves with modulated stiffness as minimizers of E_μ. In particular, we consider the following minimization problem

$$\boxed{\min_{(\rho,\gamma)\in\mathscr{P}\times\mathscr{A}} E_\mu(\rho,\gamma).} \tag{2.6}$$

In contrast to the classical Euler-Bernoulli model for elasticae [13, 17], which is a purely geometric variational problem, here the density plays an active role in the selection of the optimal geometry.

3 Existence and nonexistence

As mentioned in the Introduction, the minimization of E_0 turns out to be of limited interest. Indeed, if the integrand

$$\Phi(\rho,\kappa) = \frac{1}{2}\beta(\rho)\kappa^2$$

is strictly convex, problem (2.6) for $\mu = 0$ admits only the trivial solution

$$(\rho_0,\kappa_0) := (1,1). \tag{3.1}$$

This can be directly checked via Jensen's inequality by computing, for any $(\rho,\kappa)\in\mathscr{P}\times\mathscr{A}$,

$$E_0(\rho,\kappa) = \int_0^{2\pi} \Phi(\rho,\kappa)\,\mathrm{d}s \overset{\text{Jensen}}{\geq} 2\pi\,\Phi\left(\frac{1}{2\pi}\int_0^{2\pi}\rho\,\mathrm{d}s, \frac{1}{2\pi}\int_0^{2\pi}\kappa\,\mathrm{d}s\right) = 2\pi\,\Phi(1,1) = E_0(\rho_0,\kappa_0)$$

where the inequality is strict whenever ρ or κ are not constant, namely, whenever $(\rho,\kappa)\neq(\rho_0,\kappa_0)$. Let us mention that the integrand Φ is strictly convex if and only if

$$\beta'' > 0 \qquad \text{and} \qquad \beta''\beta > 2(\beta')^2. \tag{3.2}$$

In order to allow the complex geometrical patterning of biological shapes to possibly be described by the minimization problem (2.6), one is hence forced to dispense of (3.2), for in that case the only minimizer of E_0 (and, a fortiori E_μ) would be the trivial one (ρ_0,κ_0). In the setting of our bifurcation results, our choices for β will then fulfill

$$\beta''(\rho)\leq 0 \qquad \text{or} \qquad \beta''(\rho)\beta(\rho) \leq 2(\beta'(\rho))^2 \qquad \text{for some } \ \rho\geq 0, \tag{3.3}$$

at least in a neighborhood of the trivial state ρ_0.

On the other hand, lacking convexity of the integrand Φ, the energy E_0 fails to be weakly lower semicontinuous on $\mathscr{P}\times\mathscr{A}$ and existence of minimizers may genuinely fail. We collect a remark in this direction in the following.

Proposition 3.1 (No minimizers for E_0)**.** *Assume that*

$$\beta(0) < \beta(\rho) \quad \forall \rho > 0. \tag{3.4}$$

Then, the minimization problem (2.6) *with* $\mu = 0$ *admits no solution.*

Before moving to the proof, let us point out that condition (3.4) implies in particular that Φ is not convex. Indeed, if Φ were convex, one could take any $\rho > 0$ and $\lambda\in(0,1)$ and compute

$$\begin{aligned}\frac{1}{2}\beta(\rho)\kappa_0^2 &= \lim_{\lambda\to 1}\Phi\big(\lambda(0,\kappa_0/\lambda) + (1-\lambda)(\rho/(1-\lambda),0)\big)\\ &\leq \lim_{\lambda\to 1}\Big(\lambda\Phi(0,\kappa_0/\lambda) + (1-\lambda)\Phi(\rho/(1-\lambda),0)\Big) = \lim_{\lambda\to 1}\lambda\Phi(0,\kappa_0/\lambda) = \frac{1}{2}\beta(0)\kappa_0^2,\end{aligned}$$

contradicting (3.4). Note that the role of the value κ_0 in the latter computation is immaterial as one can argue with any $\kappa\neq 0$.

Proof of Proposition 3.1. Let us show that E_0 cannot be minimized on $\mathscr{P}\times\mathscr{A}$. We firstly remark that

$$E_0(\rho,\kappa)\overset{(3.4)}{\geq}E_0(0,\kappa)\overset{\text{Jensen}}{\geq}E_0(0,\kappa_0)\qquad\forall(\rho,\kappa)\in\mathscr{P}\times\mathscr{A}. \tag{3.5}$$

In fact, the first inequality is strict as soon as $\rho\kappa\not\equiv 0$ almost everywhere while the second one is strict as soon as κ is not constantly equal to κ_0 (recall that $\beta(0)>0$). For all $\lambda\in(0,1)$, we now define

$$\rho_\lambda(s)=\begin{cases}0 & \text{for } s\in[0,\lambda\pi]\\ \rho_0/(1-\lambda) & \text{for } s\in(\lambda\pi,\pi]\\ 0 & \text{for } s\in(\pi,(1+\lambda)\pi]\\ \rho_0/(1-\lambda) & \text{for } s\in((1+\lambda)\pi,2\pi],\end{cases}\qquad \kappa_\lambda(s)=\begin{cases}\kappa_0/\lambda & \text{for } s\in[0,\lambda\pi]\\ 0 & \text{for } s\in(\lambda\pi,\pi]\\ \kappa_0/\lambda & \text{for } s\in(\pi,(1+\lambda)\pi]\\ 0 & \text{for } s\in((1+\lambda)\pi,2\pi].\end{cases}$$

We now check that $(\rho_\lambda,\kappa_\lambda)\in\mathscr{P}\times\mathscr{A}$. Indeed,

$$\int_0^{2\pi}\rho_\lambda=2\pi(1-\lambda)\frac{\rho_0}{1-\lambda}=2\pi\rho_0=2\pi,\qquad\int_0^{2\pi}\kappa_\lambda=2\lambda\pi\frac{\kappa_0}{\lambda}=2\pi\kappa_0=2\pi.$$

Moreover, by letting $K_\lambda(s)=\displaystyle\int_0^s\kappa_\lambda(r)\,\mathrm{d}r$, namely,

$$K_\lambda(s)=\begin{cases}\kappa_0 s/\lambda & \text{for } s\in[0,\lambda\pi]\\ \kappa_0\pi & \text{for } s\in(\lambda\pi,\pi]\\ \kappa_0(s-(1-\lambda)\pi)/\lambda & \text{for } s\in(\pi,(1+\lambda)\pi]\\ \kappa_0 2\pi & \text{for } s\in((1+\lambda)\pi,2\pi],\end{cases}$$

we can compute

$$\begin{aligned}\int_0^\pi\cos\left(\int_0^s\kappa_\lambda(r)\,\mathrm{d}r\right)\mathrm{d}s&=\int_0^\pi\cos(K_\lambda(s))\,\mathrm{d}s\\ &=\int_0^{\lambda\pi}\cos(\kappa_0 s/\lambda)\,\mathrm{d}s+\int_{\lambda\pi}^{\pi}\cos(\kappa_0\pi)\,\mathrm{d}s+\int_\pi^{(1+\lambda)\pi}\cos(\kappa_0(s-(1-\lambda)\pi)/\lambda)\,\mathrm{d}s+\int_{(1+\lambda)\pi}^{2\pi}\cos(2\kappa_0\pi)\,\mathrm{d}s\\ &=\frac{\lambda}{\kappa_0}\sin(\kappa_0\pi)-\frac{\lambda}{\kappa_0}\sin 0+\cos(\kappa_0\pi)(1-\lambda)\pi+\frac{\lambda}{\kappa_0}\sin(2\kappa_0\pi)-\frac{\lambda}{\kappa_0}\sin(\kappa_0\pi)+\cos(2\kappa_0\pi)(1-\lambda)\pi\\ &=\lambda\sin\pi-\lambda\sin 0+(\cos\pi)(1-\lambda)\pi+\lambda\sin 2\pi-\lambda\sin\pi+(\cos 2\pi)(1-\lambda)\pi=0,\end{aligned}$$

and analogously

$$\begin{aligned}\int_0^{2\pi}\sin\left(\int_0^s\kappa_\lambda(r)\,\mathrm{d}r\right)\mathrm{d}s&=\int_0^{2\pi}\sin(K_\lambda(s))\,\mathrm{d}s\\ &=-\lambda\cos\pi+\lambda\cos 0+(\sin\pi)(1-\lambda)\pi-\lambda\cos 2\pi+\lambda\cos\pi+(\sin 2\pi)(1-\lambda)\pi=0.\end{aligned}$$

The latter ensures in particular that $(\rho_\lambda,\kappa_\lambda)\in\mathscr{P}\times\mathscr{A}$.

Let us now compute

$$E_0(\rho_\lambda,\kappa_\lambda)=\lambda E_0(0,\kappa_0/\lambda)+(1-\lambda)E_0(\rho/(1-\lambda),0)=\lambda E_0(0,\kappa_0/\lambda)$$

and note that $E_0(\rho_\lambda,\kappa_\lambda)\to E_0(0,\kappa_0)$ as $\lambda\to 1$. Owing to (3.5), this entails that $E_0(\rho_\lambda,\kappa_\lambda)$ is an infimizing sequence on $\mathscr{P}\times\mathscr{A}$. On the other hand, the value $E_0(0,\kappa_0)$ cannot be reached in $\mathscr{P}\times\mathscr{A}$. Indeed, assume by contradiction to have $(\rho,\kappa)\in\mathscr{P}\times\mathscr{A}$ with $E_0(\rho,\kappa)=E_0(0,\kappa_0)$. Recalling (3.5), we have that $\rho\kappa=0$ almost everywhere and $\kappa=\kappa_0$. This entails that $\rho=0$ almost everywhere so that necessarily $(\rho,\kappa)=(0,\kappa_0)$, which however does not belong to $\mathscr{P}\times\mathscr{A}$. □

Despite the lack of lower-semicontinuity and the possible nonexistence of minimizers of variational problems, in some cases information may still be retrieved by analyzing the structure of infimizing sequences, see [1]. This perspective seems however to be of little relevance here. Assume (ρ,κ) to be a minimizer of E_0 in $\mathscr{P}\times\mathscr{A}$ and let $(\rho_\#,\kappa_\#)$ denote its periodic extension to $\mathbb{R}$. Let the *fine-scaled* trajectories

$$\rho_n(s)=\rho_\#(ns),\quad\kappa_n(s)=\kappa_\#(ns)\quad\forall s\in[0,2\pi]$$

be defined. One may check that $(\rho_n,\kappa_n)\in\mathscr{P}\times\mathscr{A}$ as well and that $E_0(\rho_n,\kappa_n)=E_0(\rho,\kappa)$, so that all (ρ_n,κ_n) are minimizers (infimizing, in particular). On the other hand, (ρ_n,κ_n) weakly converges to its mean (ρ_0,κ_0). This shows that, the limiting behavior of infimizing sequences may deliver scant information, for we recover the trivial state.

These facts motivate our interest for focusing on the case $\mu>0$ in the minimization problem (2.6). In contrast to the case $\mu=0$ of Proposition 3.1, energy E_μ can be minimized in $\mathscr{P}\times\mathscr{A}$ for all $\mu>0$.

Proposition 3.2 (Existence for $\mu > 0$)**.** *Let $\mu > 0$. Then, the minimization problem* (2.6) *admits a solution.*

Proof. This is an immediate application of the Direct Method. Let $(\rho_n, \kappa_n) \in \mathscr{P} \times \mathscr{A}$ be an infimizing sequence for E_μ (such a sequence exists, for $E_\mu(\rho_0, \kappa_0) > -\infty$). We can assume with no loss of generality that $\sup E_\mu(\rho_n, \kappa_n) < \infty$. In particular, as $\beta \geq \beta_m > 0$ we have that ρ_n and κ_n are uniformly bounded in $H^1(0, 2\pi)$ and in $L^2(0, 2\pi)$, respectively. This implies, at least for a not relabeled subsequence, that $\rho_n \to \rho$ weakly in $H^1(0, 2\pi)$ and uniformly and $\kappa_n \to \kappa$ weakly in $L^2(0, 2\pi)$. We can hence pass to the limit in the relations

$$\int_0^{2\pi} \rho_n \, \mathrm{d}s = 2\pi, \quad \int_0^{2\pi} \begin{pmatrix} \cos\left(\int_0^s \kappa_n(t)\mathrm{d}t\right) \\ \sin\left(\int_0^s \kappa_n(t)\mathrm{d}t\right) \end{pmatrix} \mathrm{d}s = \begin{pmatrix} 0 \\ 0 \end{pmatrix}, \quad \int_0^{2\pi} \kappa_n \, \mathrm{d}s = 2\pi$$

and obtain that $(\rho, \kappa) \in \mathscr{P} \times \mathscr{A}$ as well.

Moreover, $\beta(\rho_n) \to \beta(\rho)$ uniformly as β is locally Lipschitz continuous. This implies that $(\beta(\rho_n))^{1/2}\kappa_n \to (\beta(\rho))^{1/2}\kappa$ weakly in $L^2(0, 2\pi)$ and lower semicontinuity ensures that $E_0(\rho, \kappa) \leq \liminf_{n\to\infty} E_0(\rho_n, \kappa_n) = \inf E_0$, so that (ρ, κ) is a solution of problem (2.6). □

The parameter μ is a datum of the problem and it is in particular related to the characteristic length scale at which ρ changes along the curve. If μ is chosen to be large compared with the length of the curve, the minimizer is again forced to be trivial. Let us make these heuristics precise in the following.

Proposition 3.3 (Trivial minimizer for μ large)**.** *For μ large enough, the trivial state (ρ_0, θ_0) is the unique solution of the minimization problem* (2.6)*.*

Proof. We structure the proof into two steps. In Step 1 we show that, for μ large, the trivial state $u_0 = (\rho_0, \theta_0)$ with $\rho_0 = 1$ and $\theta_0(t) = t$ is a strict minimizer in a neighborhood which is independent of μ. In Step 2, we prove that all minimizers converge to u_0 in the H^1 norm as $\mu \to \infty$. The combination of these two steps entails than that all minimizers necessarily coincide with u_0 for μ sufficiently large, for they are arbitrarily close to u_0 (Step 2) which is locally the unique minimizer (Step 1).

Step 1: the trivial state is a strict local minimizer. Let us check that, for μ large enough, the second variation $\delta^2 E_\mu(u_0)$ of E_μ is positive. Indeed, for the arbitrary direction $u_1 = (\rho_1, \theta_1)$ we can compute

$$\delta^2 E_\mu(u_0)(u_1, u_1) = \int_0^{2\pi} \left(\mu\dot{\rho}_1^2 + \beta(\rho_0)\dot{\theta}_1^2 + 2\beta'(\rho_0)\rho_1\dot{\theta}_1 + \frac{\beta''(\rho_0)}{2}\rho_1^2 \right) \mathrm{d}s.$$

By integrating by parts and using the Cauchy-Schwarz inequality in the third term we get

$$\begin{aligned} \delta^2 E_\mu(u_0)(u_1, u_1) \geq \mu \int_0^{2\pi} \dot{\rho}_1^2 \, \mathrm{d}s + \beta(\rho_0) \int_0^{2\pi} \dot{\theta}_1^2 \, \mathrm{d}s \\ - \left(\frac{4\beta'(\rho_0)^2}{C\beta(\rho_0)} \right)^{\frac{1}{2}} \|\dot{\rho}_1\|_{L^2(0,2\pi)} \left(C\beta(\rho_0)\right)^{\frac{1}{2}} \|\theta_1\|_{L^2(0,2\pi)} - \frac{|\beta''(\rho_0)|}{2} \int_0^{2\pi} \rho_1^2 \, \mathrm{d}s, \end{aligned}$$

where C is the Poincaré constant on $(0, 2\pi)$. Using again Poincaré's inequality to bound the second and last term in the right-hand side above, and Young's inequality for the third term we are left with

$$\delta^2 E_\mu(u_0)(u_1, u_1) \geq \left(\mu - \frac{2\beta'(\rho_0)^2}{C\beta(\rho_0)} - \frac{|\beta''(\rho_0)|}{2C} \right) \int_0^{2\pi} \dot{\rho}_1^2 \, \mathrm{d}s + \frac{\beta(\rho_0)}{2} \int_0^{2\pi} \dot{\theta}_1^2 \, \mathrm{d}s,$$

which is positive for

$$\mu > \frac{2\beta'(\rho_0)^2}{C\beta(\rho_0)} + \frac{|\beta''(\rho_0)|}{2C}.$$

As $\delta^2 E_\mu(u_0)$ is positive, u_0 minimizes E_μ on some neighborhood $U_\mu \subset \mathscr{P} \times \mathscr{A}$ for $\mu \geq \mu_0$ and for some $\mu_0 > 0$. Since E_μ is increasing in μ and $E_\mu(u_0)$ does not depend on μ, U_μ may be taken to be increasing in μ as well. Thus, u_0 minimizes E_μ on U_{μ_0} for all $\mu \geq \mu_0$.

Step 2: global minimizers converge to the trivial state. We next prove that, for any $\delta > 0$ there exists $\mu_c > 0$ such that for any $\mu > \mu_c$, any global minimizer (ρ, θ) of E_μ is such that

$$\|\rho - \rho_0\|_{L^2(0,2\pi)} + \|\theta - \theta_0\|_{L^2(0,2\pi)} \lesssim \|\dot{\rho}\|_{L^2(0,2\pi)} + \|\dot{\theta} - \dot{\theta}_0\|_{L^2(0,2\pi)} < \delta \tag{3.6}$$

where we use the sign $\lesssim$ to indicate the implicit occurrence of a constant just depending on data. In fact, we have that

$$E_\mu(\rho_0,\theta_0) \geq E_\mu(\rho,\theta) = \int_0^{2\pi} \left(\frac{1}{2}\beta(\rho)\dot\theta^2 + \frac{\mu}{2}\dot\rho^2\right) \mathrm{d}s$$
$$\geq \int_0^{2\pi} \left(\frac{1}{2}\beta_m\dot\theta^2 + \frac{\mu}{2}\dot\rho^2\right) \mathrm{d}s \geq \int_0^{2\pi} \left(\frac{1}{2}\beta_m\dot\theta_0^2 + \frac{\mu}{2}\dot\rho^2\right) \mathrm{d}s, \tag{3.7}$$

since θ_0 minimizes the Dirichlet energy $\int_0^{2\pi} \dot\theta^2 \,\mathrm{d}s$ under the conditions $\theta(0) = 0$, $\theta(2\pi) = 2\pi$. Since $E_\mu(\rho_0,\theta_0) < \infty$, both terms in the above right-hand side are bounded. We hence deduce that $\int_0^{2\pi} \dot\rho^2 \,\mathrm{d}s = O(\mu^{-1}) = o(\mu^{-1/2})$, so that there exists $\mu_1 > 0$ such that for $\mu > \mu_1$ we have $\int_0^{2\pi} \dot\rho^2 \,\mathrm{d}s < \delta/2$. Now, $\rho - \rho_0 \in H_0^1(0,2\pi)$, so that by the continuous embedding of $H_0^1(0,2\pi)$ in $L^\infty(0,2\pi)$ we have

$$\|\rho - \rho_0\|_{L^\infty(0,2\pi)} \lesssim \|\dot\rho\|_{L^2(0,2\pi)} = o(\mu^{-1/4}),$$

and, by the local Lipschitz continuity of β,

$$\|\beta(\rho) - \beta(\rho_0)\|_{L^\infty(0,2\pi)} = o(\mu^{-1/4}).$$

This allows us to refine estimate (3.7) as follows:

$$E_\mu(\rho_0,\theta_0) \geq E_\mu(\rho,\theta) \geq \int_0^{2\pi} \left(\frac{1}{2}\beta_m\dot\theta_0^2 + \frac{\mu}{2}\dot\rho^2\right) \mathrm{d}s = E_\mu(\rho_0,\theta_0) + \frac{\mu}{2}\int_0^{2\pi} \dot\rho^2 + o(\mu^{-1/4}),$$

from which we get $\lim_{\mu\to\infty} \mu \int_0^{2\pi} \dot\rho^2 \,\mathrm{d}s = 0$, and then

$$\lim_{\mu\to\infty} E_\mu(\rho,\theta) = \lim_{\mu\to\infty} \int_0^{2\pi} \frac{1}{2}\beta(\rho)\dot\theta^2 \,\mathrm{d}s = E_\mu(\rho_0,\theta_0).$$

Finally, we control

$$\left|\int_0^{2\pi} \frac{1}{2}\beta(\rho)\dot\theta^2 \,\mathrm{d}s - E_\mu(\rho_0,\theta_0)\right| = \left|\int_0^{2\pi} \frac{\beta(\rho_0)}{2}(\dot\theta^2 - \dot\theta_0^2)\mathrm{d}s + o(\mu^{-1/4})\right|,$$

so to prove that $\lim_{\mu\to\infty} \int_0^{2\pi} \dot\theta^2 \,\mathrm{d}s = \lim_{\mu\to\infty} \int_0^{2\pi} \dot\theta_0^2 \,\mathrm{d}s = 2\pi$. This is enough to conclude that

$$\lim_{\mu\to\infty} \|\dot\theta - \dot\theta_0\|_{L^2(0,2\pi)} = 0.$$

We can then choose μ_2 such that, for $\mu > \mu_2$, $\|\dot\theta - \dot\theta_0\|_{L^2(0,2\pi)} < \delta/2$ and set $\mu_c = \max\{\mu_1,\mu_2\}$ for which the second inequality in (3.6) holds. The first inequality follows from Poincaré's inequality. □

We present now a symmetry result which will turn out useful later on, when interpreting the numerical findings.

Proposition 3.4. *If (ρ,θ) is a local minimizer of E_μ for β, then $(2\rho_0 - \rho, \theta)$ is a local minimizer of E_μ for $\tilde\beta$, defined as $\tilde\beta(\rho) = \beta(2\rho_0 - \rho)$.*

Proof. The integrand is unchanged by this transformation, so that the first and second variations of E_μ at (ρ,θ) and $(2\rho_0 - \rho,\theta)$ when considering respectively β and $\tilde\beta$ are identical. □

4 Bifurcation analysis

We study the *local bifurcation structure* of solutions from the trivial solution (ρ_0,θ_0) as the bifurcation parameter μ decreases, i.e. in the limit of vanishing regularization (see Figure 1.1). Our argument is based on a perturbation approach, the theoretical background being bifurcation theory from simple eigenvalues, see [7]. The bifurcation analysis gives criteria on the material parameters defining the bending coefficient β, for which nontrivial solutions are expected.

4.1 Euler-Lagrange equations

Stationary points of the energy E_μ in $\mathscr{P} \times \mathscr{A}$ are solutions to the *Euler-Lagrange equations*,

$$\mu\ddot{\rho} - \frac{1}{2}\,\beta'(\rho)\,\dot{\theta}^2 = \lambda_M, \tag{4.1}$$

$$\frac{d}{ds}\left(\beta(\rho)\,\dot{\theta}\right) = -\lambda_x \sin\theta + \lambda_y \cos\theta, \tag{4.2}$$

along with the *boundary conditions* (ensuring periodicity of ρ and $\kappa = \dot{\theta}$)

$$\rho\big|_0^{2\pi} = 0, \quad \dot{\rho}\big|_0^{2\pi} = 0, \quad \theta\big|_0^{2\pi} = 2\pi, \quad \dot{\theta}\big|_0^{2\pi} = 0, \tag{4.3}$$

the mass and closedness *constraints*

$$\int_0^{2\pi} \rho(s)\,\mathrm{d}s = 2\pi \quad \text{and} \quad \int_0^{2\pi} \begin{pmatrix}\cos\theta \\ \sin\theta\end{pmatrix} \mathrm{d}s = \begin{pmatrix}0\\0\end{pmatrix}, \tag{4.4}$$

and the extra requirement eliminating rotation invariance

$$\theta(0) = 0. \tag{4.5}$$

The real numbers λ_M, λ_x, and λ_y are the *Lagrange multipliers* arising from stationarity of E_μ under the constraints (4.4). In particular, stationary points of E_μ on $\mathscr{P} \times \mathscr{A}$ for $\mu > 0$ fulfill indeed $(\rho, \theta) \in H^2(0, 2\pi)^2$ as well as the periodicity of $\dot{\rho}$ and $\dot{\theta}$. In fact, regularity can be bootstrapped if β is more regular and (ρ, θ) can be proved to be in C^∞ if β also is.

We note that the seven constraint equations (4.3)–(4.4) are sufficient to determine the four parameters in the general solution of the two second-order ODEs (4.1)–(4.2) and the three scalars $\lambda_M, \lambda_x, \lambda_y$.

In the remainder of this work, we restrict to a *quadratic bending rigidity* model, more precisely, to $\beta \in C^\infty(\mathbb{R})$ with zero third- and forth- order Taylor coefficients at ρ_0. For simplicity, we consider

$$\beta(\rho) = \beta_0 \left(1 + m(\rho - \rho_0) + \frac{h}{2}(\rho - \rho_0)^2\right) \tag{4.6}$$

with $\beta_0 > 0$ and $m, h \in \mathbb{R}$. We have $\beta'(\rho) = \beta_0\,(m + h(\rho - \rho_0))$ and $\beta''(\rho) = \beta_0 h$, whence with

$$\beta_0 = \beta(\rho_0), \quad \beta_0' := \beta'(\rho_0), \quad \beta_0'' := \beta''(\rho_0)$$

we get

$$m = \beta_0'/\beta_0 \quad \text{and} \quad h = \beta_0''/\beta_0.$$

We note that $\beta_0 > 0$ guarantees that $\beta(\rho) > 0$ for all ρ in a neighborhood of ρ_0. Recall that we avoid the strict convexity conditions (3.2) for β, namely $h > 0$ and $\beta''\beta > 2(\beta')^2$. Therefore we will need to assume that $h \le 0$ or that there exists $\rho \in \mathbb{R}$ such that $\beta''\beta \le 2(\beta')^2$. As evaluation at ρ_0 gives $h\beta_0^2 = \beta_0''\beta_0 \le 2(\beta_0')^2 = 2m^2\beta_0^2$, this is the case if

$$h \le 2m^2. \tag{4.7}$$

Finally we can scale the model to

$$\beta_0 = 1, \tag{4.8}$$

which in particular implies that $\beta(\rho) = 1 + m(\rho - 1) + \frac{h}{2}(\rho - 1)^2$. Let us emphasize that the restriction to a bending rigidity of the form (4.6) will not affect the linearized system, but simplifies our bifurcation analysis by reducing the stiffness model parameters to the two real numbers m and h.

4.2 Linearization around the trivial state

The constrained nonlinear Euler-Lagrange equations (4.1)–(4.5) are an μ-dependent system for

$$\bar{u} := (\rho, \theta, \lambda_M, \lambda_x, \lambda_y) \in H^2(0, L)^5,$$

where the Lagrange multipliers $\lambda_M, \lambda_x, \lambda_y$ are treated as constant functions. First we show that the trivial state given by constant density distribution on the circle (ρ_0, θ_0) solves the Euler-Lagrange system at any regularization level $\mu \ge 0$.

Proposition 4.1 (**Trivial state**). *The pair* $(\rho_0, \theta_0)\colon [0, L] \to \mathbb{R}^2$ *given in* (3.1)*, with Lagrange multipliers*

$$\lambda_x = 0 =: \lambda_{x0}, \qquad \lambda_y = 0 =: \lambda_{y0}, \qquad \lambda_M = -\frac{1}{2}\,\beta'(\rho_0)\,\kappa_0^2 =: \lambda_{M0}, \tag{4.9}$$

satisfies the system (4.1)–(4.4) *for all* $\mu \geq 0$

Proof. Since $\dot\rho_0(s) = 0$ and $\dot\theta_0(s) = \kappa_0 = 2\pi/L$, the trivial solution satisfies all conditions (4.3)–(4.5). The equations (4.1) and (4.2) reduce to $-\frac{1}{2}\,\beta'(\rho_0)\,\dot\theta_0^2 = \lambda_M$ and $0 = -\lambda_x \sin\theta_0 + \lambda_y \cos\theta_0$, which with $\theta_0(s) = \kappa_0 s$ for $s \in [0, L]$ yield $\lambda_M = \lambda_{M0}$ and $\lambda_x = \lambda_y = 0$. □

Next we consider the linearization around the trivial solution $\bar u_0 := (\rho_0, \theta_0, \lambda_{M0}, \lambda_{x0}, \lambda_{y0})$. The linearized system for $\bar u_1 := (\rho_1, \theta_1, \lambda_{M1}, \lambda_{x1}, \lambda_{y1})$ is obtained by first-order expansion of the equations when one inserts the first-order perturbation ansatz

$$\bar u = \bar u_0 + A\bar u_1 + O(A^2) \qquad \text{with} \qquad A \to 0.$$

With normalization, recalling that $\dot\theta_0 = \kappa_0 = 1$ and $\lambda_{x0} = \lambda_{y0} = 0$, we obtain the **linearized system** consisting of the linearized Euler-Lagrange equations

$$\mu\ddot\rho_1 - m\,\dot\theta_1 - \frac{h}{2}\,\rho_1 = \lambda_{M1}, \tag{4.10}$$

$$\frac{d}{ds}\left(\dot\theta_1 + m\,\rho_1\right) = -\lambda_{x1}\sin + \lambda_{y1}\cos, \tag{4.11}$$

the linearized boundary conditions

$$\rho_1\big|_0^{2\pi} = 0, \quad \dot\rho_1\big|_0^{2\pi} = 0, \quad \theta_1\big|_0^{2\pi} = 0, \quad \dot\theta_1\big|_0^{2\pi} = 0, \tag{4.12}$$

the linearized mass and closedness constraints

$$\int_0^{2\pi} \rho_1(s)\,\mathrm{d}s = 0 \quad \text{and} \quad \int_0^{2\pi} \begin{pmatrix} -\sin(s) \\ \cos(s) \end{pmatrix} \theta_1(s)\mathrm{d}s = \begin{pmatrix} 0 \\ 0 \end{pmatrix}, \tag{4.13}$$

and the linearized extra condition eliminating rotational invariance,

$$\theta_1(0) = 0. \tag{4.14}$$

We notice that the linearized closedness constraint states that θ_1 must have zero first Fourier coefficients, which is consistent with the Four Vertex Theorem (see Section 2).

Next, we discuss solvability of (4.10)–(4.14) depending on the values of m, h and μ. In particular, there exist regimes with different coupling behavior of the shape- and density-perturbations θ_1 and ρ_1:

Proposition 4.2 (**Solution of the linearized system**). *A nonzero solution of the linearized system* (4.10)–(4.14) *only exists in the following cases:*

- Case 0 (**Direct coupling**): *If* $h < 2m^2$*,* $m \neq 0$*, and* $\mu = \frac{1}{j^2}\left(m^2 - \frac{h}{2}\right) \neq -\frac{h}{2}$ *for some* $j \in \mathbb{Z}$ *with* $|j| \geq 2$*, then with* $a_1, s_1 \in \mathbb{R}$*,*

  $$\begin{aligned} &\rho_1(s) = -a_1\,\cos(js - s_1), \qquad && \lambda_{x1} = \lambda_{y1} = \lambda_{M1} = 0, \\ &\theta_1(s) = \tfrac{a_1 m}{j}(\sin(js - s_1) + \sin(s_1)). \end{aligned}$$

  In particular, $\dot\theta_1(s) = -m\rho_1(s) = a_1 m\,\cos(js - s_1)$*.*

- Case 1 (**No coupling**):

  Case 1.0: *If* $h < 0$*,* $m = 0$*, and* $\mu = -\frac{1}{j^2}\frac{h}{2}$ *for some* $j \in \mathbb{Z} \setminus \{0\}$*, then with* $a_1, s_1 \in \mathbb{R}$*,*

  $$\begin{aligned} &\rho_1(s) = -a_1\,\cos(js - s_1), \qquad && \lambda_{x1} = \lambda_{y1} = \lambda_{M1} = 0, \\ &\theta_1(s) = 0. \end{aligned}$$

  Case 1.1: *If* $h < 0$*,* $m \neq 0$*, and* $\mu = -\frac{h}{2} \neq \frac{1}{j^2}\left(m^2 - \frac{h}{2}\right)$ *for all* $j \in \mathbb{Z}$ *with* $|j| \geq 2$*, then with* $b_1, \tilde s_1 \in \mathbb{R}$*,*

  $$\begin{aligned} \rho_1(s) &= -b_1\,\cos(s - \tilde s_1) && \lambda_{x1} = -b_1 m\cos(\tilde s_1), \\ &= \tfrac{1}{m}(\lambda_{x1}\cos(s) + \lambda_{y1}\sin(s)), && \lambda_{y1} = -b_1 m\sin(\tilde s_1), \\ \theta_1(s) &= 0, && \lambda_{M1} = 0. \end{aligned}$$

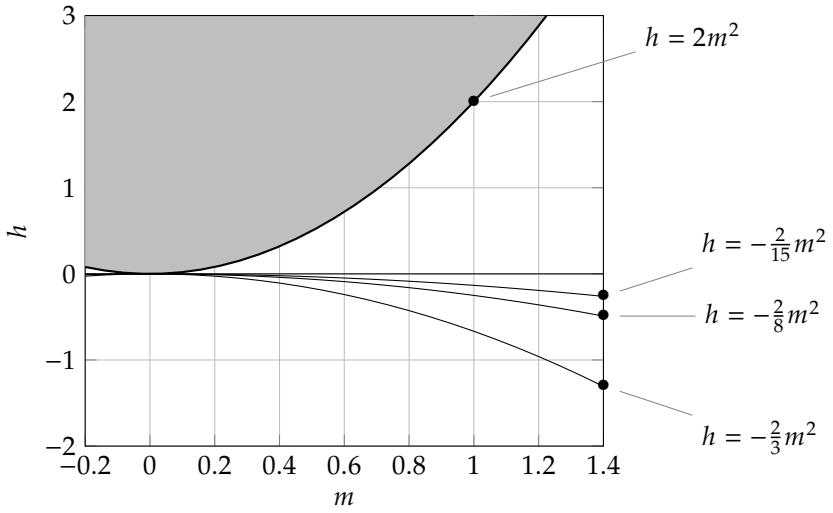

Figure 4.1: Admissible regions of the (m, h)-plane according to Proposition 4.2: Nontrivial solutions of the linearized problem exist for $h < 2m^2$ with $m \neq 0$ (Case 0), $h < 0$ (Case 1), or on the parabolas $h = -\frac{2m^2}{j^2-1} \neq 0$ for some $|j| \geq 2$ (Case 2). Above the parabolas, Case 0 bifurcates already at larger μ than Case 1, see (4.15).

- Case 2 (**Asymmetric coupling**): *If $h < 0$, $m \neq 0$, and $\mu = -\frac{h}{2} = \frac{1}{j^2}\left(m^2 - \frac{h}{2}\right)$ for some $j \in \mathbb{Z}$ with $|j| \geq 2$, then with $a_1, b_1, s_1, \tilde{s}_1 \in \mathbb{R}$,*

$$\begin{aligned} \rho_1(s) &= -a_1 \cos(js - s_1) - b_1 \cos(s - \tilde{s}_1) && \lambda_{x1} = -b_1 m \cos(\tilde{s}_1), \\ &= -a_1 \cos(js - s_1) + \tfrac{1}{m}(\lambda_{x1}\cos(s) + \lambda_{y1}\sin(s)), && \lambda_{y1} = -b_1 m \sin(\tilde{s}_1), \\ \theta_1(s) &= \tfrac{a_1 m}{j}\big(\sin(js - s_1) + \sin(s_1)\big), && \lambda_{M1} = 0. \end{aligned}$$

  In particular, $\dot{\theta}_1(s) = a_1 m \cos(js - s_1)$.

Solutions in Cases 0 and 2 are ellipsoidal ($|j| = 2$) or higher-mode deviations from the circle, where density perturbations couple to the shape. Case 1 gives uncoupled solutions, as they are circles with variable density. Asymmetric coupling (Case 2) is only possible for the specific parameter combinations $\frac{1}{j^2}(m^2 - \frac{h}{2}) = -\frac{h}{2}$ for some $j \in \mathbb{Z}$ with $|j| \geq 2$, that is,

$$h \in \{-\tfrac{2m^2}{j^2-1} : j \in \mathbb{Z},\ |j| \geq 2\} = \{-\tfrac{2m^2}{3}, -\tfrac{2m^2}{8}, -\tfrac{2m^2}{15}, \ldots\},$$

which are excluded from the range of Case 0 and 1 (see Figure 4.1). The parameter ranges in all three cases are in accordance with the nonconvexity condition $h \leq 2m^2$, see (4.7).

The case of parameters for which the solution possesses the largest critical μ will bifurcate first from the trivial branch. In the common region $h < 0$ of Cases 0, 1, 2, we have

$$\mu_{\text{Case 0}} > \mu_{\text{Case 1}} \iff \tfrac{1}{j^2}(m^2 - \tfrac{h}{2}) > -\tfrac{h}{2} \iff h > -\tfrac{2m^2}{j^2-1}. \tag{4.15}$$

In particular, restricting to the lowest mode $|j| = 2$, if $-\frac{2m^2}{3} < h < 2m^2$ then the solution first bifurcates as Case 0, if $h < -\frac{2m^2}{3}$ it bifurcates as Case 1, and if $h = -\frac{2m^2}{3}$ it is Case 2.

The amplitude parameters a_1 and b_1 in Cases 0 and 1, which are of codimension-one, will be specified in Section 4.4 from solvability of higher-order perturbations of the system, see (4.30), (4.33) and (4.35) respectively. The degenerate Case 2 features two amplitude parameters.

We conclude this section with the proof of Proposition 4.2:

Proof. In the following we write the linearized mass and closedness constraints in terms of Fourier coefficients, namely $\widehat{\rho}_1(0) = 0$ and $\widehat{\theta}_1(\pm 1) = 0$ respectively, with the k-th Fourier coefficient of a function $f \in L^1(0, L)$ given by $\widehat{f}(k) := \frac{1}{L}\int_0^L f(s)\, e^{-\mathrm{i}k\kappa_0 s}\mathrm{d}s$ for $k \in \mathbb{Z}$.

Integrating the first Euler-Lagrange equation $\mu\ddot{\rho}_1 - m\,\dot{\theta}_1 - \frac{1}{2}\,h\,\rho_1 = \lambda_{M1}$ (4.10) from 0 to 2π gives

$$\mu \underbrace{\dot{\rho}_1\Big|_0^{2\pi}}_{=0} - m \underbrace{\theta_1\Big|_0^{2\pi}}_{=0} - \frac{1}{2}\,h \underbrace{\int_0^{2\pi} \rho_1}_{=2\pi\widehat{\rho}_1(0)=0} = 2\pi\,\lambda_{M1} \quad \Longrightarrow \quad \lambda_{M1} = 0.$$

Then (4.10) reads $\mu\ddot{\rho}_1 - m\,\dot{\theta}_1 - \frac{1}{2}\,h\,\rho_1 = 0$ and with the closedness constraint $\widehat{\theta}_1(\pm 1) = 0$, the first Fourier coefficients reduce to

$$-\left(\mu + \frac{h}{2}\right)\widehat{\rho}_1(\pm 1) = \mp m\,\mathrm{i}\,\widehat{\theta}_1(\pm 1) = 0. \tag{4.16}$$

Integration of the second Euler-Lagrange equation $\frac{d}{ds}(\dot{\theta}_1 + m\,\rho_1) = -\lambda_{x1}\sin + \lambda_{y1}\cos$ (4.11) results in $\dot{\theta}_1 + m\,\rho_1 = \lambda_{x1}\cos + \lambda_{y1}\sin + c$ with integration constant $c = 0$ because

$$2\pi\,c = \dot{\theta}_1\Big|_0^{2\pi} + m\,\rho_1\Big|_0^{2\pi} - \lambda_{x1}\cos\Big|_0^{2\pi} - \lambda_{y1}\sin\Big|_0^{2\pi} = 0.$$

Thus

$$\dot{\theta}_1 = -m\,\rho_1 + \lambda_{x1}\cos + \lambda_{y1}\sin\,. \tag{4.17}$$

Insertion in the first Euler-Lagrange equation (4.10) leads to $\mu\ddot{\rho}_1 - m\,(-m\,\rho_1 + \lambda_{x1}\cos + \lambda_{y1}\sin) - \frac{1}{2}\,h\,\rho_1 = 0$, that is,

$$\mu\ddot{\rho}_1 + \Big(m^2 - \frac{h}{2}\Big)\rho_1 = m\,\lambda_{x1}\cos + m\,\lambda_{y1}\sin\,. \tag{4.18}$$

Writing $\lambda_{x1}\cos(s) + \lambda_{y1}\sin(s) = \frac{1}{2}\,\lambda_{x1}(e^{\mathrm{i}s} + e^{-\mathrm{i}s}) - \frac{\mathrm{i}}{2}\,\lambda_{y1}(e^{\mathrm{i}s} - e^{-\mathrm{i}s}) = \frac{1}{2}\,(\lambda_{x1} - \mathrm{i}\lambda_{y1})\,e^{\mathrm{i}s} + \frac{1}{2}\,(\lambda_{x1} + \mathrm{i}\lambda_{y1})\,e^{-\mathrm{i}s}$ shows $(\lambda_{x1}\cos + \lambda_{y1}\sin)\widehat{\ }(\pm 1) = \frac{1}{2}\,(\lambda_{x1} \mp \mathrm{i}\lambda_{y1})$, whence the Fourier coefficients of order $j \in \mathbb{Z}$ of (4.18) are given by

$$\underbrace{\Big(-j^2\mu + m^2 - \frac{h}{2}\Big)}_{=:\,\mathit{II}_j}\widehat{\rho}_1(j) = \begin{cases} \frac{m}{2}\,(\lambda_{x1} \mp \mathrm{i}\lambda_{y1})\,, & j = \pm 1, \\ 0, & |j| \geq 2. \end{cases} \tag{4.19}$$

Together with $\underbrace{(\mu + \frac{h}{2})}_{=:\,I}\widehat{\rho}_1(\pm 1) = 0$ (4.16), this gives rise to distinguish the cases

- $I \neq 0$ and $\exists\, j \in \mathbb{Z},\ |j| \geq 2:\ \mathit{II}_j = 0.$
  $\iff h < 2m^2,\ \mu = \frac{1}{j^2}\left(m^2 - \frac{h}{2}\right) \neq -\frac{h}{2}$ for some $j \in \mathbb{Z},\ |j| \geq 2;$
  $\overset{m=0}{\iff} h < 0,\ \mu = -\frac{1}{j^2}\,\frac{h}{2}$ for some $j \in \mathbb{Z},\ |j| \geq 2,$
- $I = 0$, and $\forall\, j \in \mathbb{Z},\ |j| \geq 2:\ \mathit{II}_j \neq 0.$
  $\iff h < 0,\ \mu = -\frac{h}{2} \neq \frac{1}{j^2}\left(m^2 - \frac{h}{2}\right)$ for all $j \in \mathbb{Z},\ |j| \geq 2;$
  $\overset{m=0}{\iff} h < 0,\ \mu = -\frac{h}{2},$
- $I = 0$ and $\exists\, j \in \mathbb{Z},\ |j| \geq 2:\ \mathit{II}_j = 0.$
  $\iff h < 0,\ m \neq 0,\ \mu = \frac{1}{j^2}\left(m^2 - \frac{h}{2}\right) = -\frac{h}{2}$ for some $j \in \mathbb{Z},\ |j| \geq 2;$
  here, $m \neq 0$ follows from $h < 0$, $m^2 = (1 - j^2)\frac{h}{2}$, and $|j| \geq 2$.

We arrive at the following Cases 0, 1, 2, where Case 1.0 combines the two situations with $m = 0$:

Case 0: $h < 2m^2,\ m \neq 0,\ \mu = \frac{1}{j^2}\left(m^2 - \frac{h}{2}\right) \neq -\frac{h}{2}$ for some $j \in \mathbb{Z},\ |j| \geq 2.$

Case 1.0: $h < 0,\ m = 0,\ \mu = -\frac{1}{j^2}\,\frac{h}{2}$ for some $j \in \mathbb{Z},\ |j| \geq 1;$

Case 1.1: $h < 0,\ m \neq 0,\ \mu = -\frac{h}{2} \neq \frac{1}{j^2}\left(m^2 - \frac{h}{2}\right)$ for all $j \in \mathbb{Z},\ |j| \geq 2.$

Case 2: $h < 0,\ m \neq 0,\ \mu = \frac{1}{j^2}\left(m^2 - \frac{h}{2}\right) = -\frac{h}{2}$ for some $j \in \mathbb{Z},\ |j| \geq 2.$

• Solution in Case 0: As $I = \mu + \frac{h}{2} \neq 0$, we know

$$\widehat{\rho}_1(\pm 1) = 0 \tag{4.20}$$

from $(\mu + \frac{h}{2})\widehat{\rho}_1(\pm 1) = 0$ (4.16). By $(-\mu + m^2 - \frac{h}{2})\widehat{\rho}_1(\pm 1) = \frac{m}{2}(\lambda_{x1} \mp \mathrm{i}\lambda_{y1})$ (4.19) and $m \neq 0$, this implies

$$\lambda_{x1} = \lambda_{y1} = 0.$$

Then (4.18) reduces to the homogeneous ODE

$$\mu\ddot{\rho}_1 + (m^2 - \tfrac{h}{2})\rho_1 = 0,$$

which with $II_j = -j^2\mu + m^2 - \frac{h}{2} = 0$ for some $j \in \mathbb{Z}$ with $|j| \geq 2$ simply reads

$$\mu(\ddot{\rho}_1 + j^2\rho_1) = 0.$$

The solution satisfying the constraints $\rho_1\big|_0^{2\pi} = \dot{\rho}_1\big|_0^{2\pi} = 0$, $\widehat{\rho}_1(0) = 0$ is given by

$$\rho_1(s) = \rho_{1,\mathrm{hom}}(s) = -a_1\cos(js - s_1), \quad a_1, s_1 \in \mathbb{R}$$

Note that the condition $\widehat{\rho}_1(\pm 1) = 0$ (4.20) is consistent with the restriction $|j| \geq 2$. With $\lambda_{y1} = \lambda_{x1} = 0$ (4.17) reduces to

$$\dot{\theta}_1 = -m\rho_1.$$

Consequently we obtain

$$\theta_1(s) = \tfrac{a_1 m}{j}\,\sin(js - s_1) + C$$

which fulfills the constraints $\dot{\theta}_1\big|_0^{2\pi} = 0$, and $\widehat{\theta}_1(1) = 0$. Next, we determine the integration constant C from $\theta_1(0) = \theta_1(2\pi) = 0$:

$$\theta_1(0) = -\tfrac{a_1 m}{j}\,\sin(s_1) + C = 0 \quad \Longrightarrow \quad C = \tfrac{a_1 m}{j}\,\sin(s_1)$$

Thus the solution reads $\theta_1(s) = \frac{a_1 m}{j}\Big(\sin(js - s_1) + \sin(s_1)\Big)$.

• Solution in Case 1: We first consider Case 1.0, where $m = 0$ with $\mu = -\frac{1}{j^2}\frac{h}{2}$ for some $j \in \mathbb{Z}$, $|j| \geq 1$. As $m = 0$, the linearized system (4.10), (4.11) is decoupled:

$$\begin{aligned} \mu\ddot{\rho}_1 - \frac{h}{2}\,\rho_1 &= \lambda_{M1}, \\ \ddot{\theta}_1 &= -\lambda_{x1}\sin + \lambda_{y1}\cos\,. \end{aligned}$$

The first Euler-Lagrange equation (with $\lambda_{M1} = 0$) or the ODE (4.18) then reduces to

$$\mu(\ddot{\rho}_1 + j^2\rho_1) = 0$$

which possesses the solution

$$\rho_1(s) = \rho_{1,\mathrm{hom}}(s) = -a_1\cos(js - s_1), \quad a_1, s_1 \in \mathbb{R}.$$

Since $\dot{\theta}_1 = \lambda_{x1}\cos + \lambda_{y1}\sin$ by the second Euler-Lagrange equation or by (4.17), we get

$$\theta_1 = \lambda_{x1}\sin - \lambda_{y1}\cos + C.$$

But $\widehat{\theta}_1(\pm 1)$ implies $\lambda_{x1} = \lambda_{y1} = 0$, and by $\theta_1(0) = \theta_1(2\pi) = 0$ we have $C = 0$, which results in

$$\theta_1(s) = 0.$$

In Case 1.1 where $m \neq 0$, having $m^2 - \frac{h}{2} = j^2\mu$ for some $j \in \mathbb{Z} \setminus \{0, \pm 1\}$ is excluded by $II_j \neq 0$. Therefore the ODE (4.18)

$$\mu\ddot{\rho}_1 + (m^2 - \tfrac{h}{2})\rho_1 = m\,\lambda_{x1}\cos + m\,\lambda_{y1}\sin$$

only has the trivial solution of the homogeneous equation. The solution of the inhomogeneous equation reads

$$\rho_1(s) = -b_1\cos(s - \tilde{s}_1), \quad b_1, \tilde{s}_1 \in \mathbb{R}$$

for

$$\lambda_{x1} = -b_1 m\cos(\tilde{s}_1), \qquad \lambda_{y1} = -b_1 m\sin(\tilde{s}_1).$$

Indeed, by inserting in (4.18) with $\mu = -\frac{h}{2}$ and $\cos(s - \tilde{s}_1) = \cos(\tilde{s}_1)\cos(s) + \sin(\tilde{s}_1)\sin(s)$ shows

$$\begin{aligned} \mu\ddot{\rho}_1 + (m^2 - \tfrac{h}{2})\rho_1 &= (-\mu + m^2 - \tfrac{h}{2})\rho_1 \\ &= m^2\rho_1 = -b_1 m^2\cos(\cdot - \tilde{s}_1) \\ &= -b_1 m^2\cos(\tilde{s}_1)\cos - b_1 m^2\sin(\tilde{s}_1) = m\,\lambda_{x1}\cos + m\,\lambda_{y1}\sin\,. \end{aligned}$$

Note that the solution ρ_1 is consistent with $\widehat{\rho}_1(\pm j) = 0$ for $|j| \geq 2$ by (4.19) as well as the mass constraint $\widehat{\rho}_1(0) = 0$. Finally, (4.17) gives

$$\begin{aligned} \dot{\theta}_1 &= -m\,\rho_1 + \lambda_{x1}\cos + \lambda_{y1}\sin \\ &= m b_1\cos(\cdot - \tilde{s}_1) - b_1 m\cos(\tilde{s}_1)\cos - b_1 m\sin(\tilde{s}_1)\sin\, = 0 \end{aligned}$$

showing that $\theta_1(s) = C = 0$.

• Solution in Case 2: As $m^2 - \frac{h}{2} = j^2\mu$ for some $j \in \mathbb{Z}$ with $|j| \geq 2$, the operator of the ODE (4.18)

$$\mu\ddot{\rho}_1 + \Big(m^2 - \frac{h}{2}\Big)\rho_1 = m\,\lambda_{x1}\cos + m\,\lambda_{y1}\sin$$

has the nontrivial kernel $\rho_{1,\mathrm{hom}}(s) = -a_1\cos(js - s_1)$ for $a_1, s_1 \in \mathbb{R}$. Consequently, the solution reads

$$\rho_1(s) = -a_1\cos(js - s_1) - b_1\cos(s - \tilde{s}_1), \quad a_1, b_1, s_1, \tilde{s}_1 \in \mathbb{R}$$

for

$$\lambda_{x1} = -b_1 m\cos(\tilde{s}_1), \qquad \lambda_{y1} = -b_1 m\sin(\tilde{s}_1),$$

which can be verified by insertion: Taking into account that $\mu = \frac{1}{j^2}\left(m^2 - \frac{h}{2}\right) = -\frac{h}{2}$ gives

$$\begin{aligned}\mu\ddot{\rho}_1(s) + (m^2 - \tfrac{h}{2})\rho_1(s) = &\underbrace{(-j^2\mu + m^2 - \tfrac{h}{2})}_{=0}(-a_1\cos(js - s_1)) \\ &+ \underbrace{(\mu + m^2 - \tfrac{h}{2})}_{=m^2}(-b_1\cos(s - \tilde{s}_1)) = -b_1 m^2\cos(s - \tilde{s}_1)\end{aligned}$$

and then one can proceed as in Case 1 for $m \neq 0$. Moreover, (4.17) gives

$$\begin{aligned}\dot{\theta}_1(s) &= -m\,\rho_1(s) + \lambda_{x1}\cos(s) + \lambda_{y1}\sin(s) \\ &= m(a_1\cos(js - s_1) + b_1\cos(s - \tilde{s}_1)) - b_1 m\cos(\tilde{s}_1)\cos(s) - b_1 m\sin(\tilde{s}_1)\sin(s) \\ &= m a_1\cos(js - s_1).\end{aligned}$$

It follows that $\theta_1(s) = \frac{m a_1}{j}\sin(js - s_1) + C$. With the constraints $\theta_1(0) = \theta_1(2\pi) = 0$ we get

$$\theta_1(0) = -\tfrac{a_1 m}{j}\sin(s_1) + C = 0 \quad \Longrightarrow \quad C = \tfrac{a_1 m}{j}\sin(s_1)$$

and the solution reads $\theta_1(s) = \frac{a_1 m}{j}\big(\sin(js - s_1) + \sin(s_1)\big)$. □

4.3 Higher-order perturbations

In order to investigate the local bifurcation structure of solutions $\bar{u} = (\rho, \theta, \lambda_M, \lambda_x, \lambda_y)$ of the system as the parameter μ changes, we systematically derive higher-order perturbations of the nonlinear Euler-Lagrange equations (4.1), (4.2) with boundary conditions (4.3) and constraints (4.4), (4.5).

As we are interested in the solution behavior for μ in the vicinity of the critical bifurcation parameter μ_0, the difference $\mu_0 - \mu$ is small. In order to approach μ_0 from both sides, we introduce

$$\sigma A^2 := \mu_0 - \mu \qquad \text{with} \qquad \sigma = \pm 1.$$

We thus consider the perturbation ansatz

$$\bar{u} = \bar{u}_0 + A\bar{u}_1 + A^2\bar{u}_2 + A^3\bar{u}_3 + O(A^4), \qquad \mu = \mu_0 - \sigma A^2 \tag{4.21}$$

with $A \to 0$. The value μ_0 is the one for the first-order solution $\bar{u}_1 = (\rho_1, \theta_1, \lambda_{M1}, \lambda_{x1}, \lambda_{y1})$ given in Proposition 4.2. Accordingly, we will have to consider $\bar{u}_1$ and μ_0 in the three regimes of the Cases 0, 1, 2. The different scaling of the perturbations of the solution u and of the bifurcation parameter μ is tailored to detecting a pitchfork bifurcation at μ_0, which will be *supercritical* if $\sigma = 1$ and *subcritical* if $\sigma = -1$.

Remark 4.3 (**Bifurcation diagram for classical elasticae**)**.** The ansatz (4.21) is motivated by the bifurcation diagram for classical elasticae (e.g. [14, Ch. 7]), which are solutions of $E\ddot{\theta} + \lambda\sin\theta = 0$. The diagram has the shape of nested supercritical pitchforks, that is, the solution branches are translated square-root functions of the parameter λ/E, which are located at the discrete eigenvalues $\lambda/E = (2\pi j/L)^2$, $j \in \mathbb{Z}\setminus\{0\}$ of the linearized operator $\frac{d^2}{dt^2} + \lambda/E$ on $H^2(0, L)$ (cf. Figure 1.1). This suggests that perturbations of the bifurcation parameter $1/\mu$ should scale quadratically. For μ_0 fixed and the perturbation parameter A going to zero, we have

$$\frac{1}{\mu} = \frac{1}{\mu_0 - A^2} = \frac{1}{\mu_0}\frac{1}{1 - A^2/\mu_0} = \frac{1}{\mu_0}\left(1 + A^2/\mu_0\right) + O(A^4/\mu_0^2) = \frac{1}{\mu_0} + \frac{A^2}{\mu_0^2} + O(A^4/\mu_0^2).$$

Therefore, a quadratically scaled perturbation of $1/\mu$ corresponds to $\mu = \mu_0 - A^2$ (in the supercritical regime).

The Euler-Lagrange equation (4.1), namely $\mu\ddot{\rho} - \frac{1}{2}\beta'(\rho)\,\dot{\theta}^2 = \lambda_M$, imply $-m/2 = \lambda_{M0}$ at order zero as well as the following hierarchy of perturbations:

$$\begin{aligned}
&\mu_0\,\ddot{\rho}_1 - m\dot{\theta}_1 - \frac{h}{2}\rho_1 = \lambda_{M1}, \quad \text{(cf. (4.10))},\\
&\mu_0\,\ddot{\rho}_2 - m\Big(\dot{\theta}_2 + \frac{1}{2}\dot{\theta}_1^2\Big) - \frac{h}{2}\Big(\rho_2 + 2\rho_1\dot{\theta}_1\Big) = \lambda_{M2}, \qquad (4.22)\\
&\mu_0\,\ddot{\rho}_3 - \sigma\ddot{\rho}_1 - m\Big(\dot{\theta}_3 + \dot{\theta}_1\dot{\theta}_2\Big) - \frac{h}{2}\Big(\rho_3 + 2\rho_2\dot{\theta}_1 + 2\rho_1\dot{\theta}_2 + \rho_1\dot{\theta}_1^2\Big) = \lambda_{M3}. \qquad (4.23)
\end{aligned}$$

The perturbations of the Euler-Lagrange equation (4.2), namely $\frac{d}{ds}\Big(\beta(\rho)\,\dot{\theta}\Big) = -\lambda_x\sin(\theta) + \lambda_y\cos(\theta)$, are given by

$$\begin{aligned}
&\frac{d}{ds}\Big(\dot{\theta}_1 + m\rho_1\Big) = -\lambda_{x1}\sin + \lambda_{y1}\cos, \quad \text{(cf. (4.11))},\\
&\frac{d}{ds}\Big(\dot{\theta}_2 + m\rho_2 + m\rho_1\dot{\theta}_1 + \frac{h}{2}\rho_1^2\Big) = -\lambda_{x2}\sin + \lambda_{y2}\cos - \theta_1(\lambda_{x1}\cos + \lambda_{y1}\sin), \qquad (4.24)\\
&\frac{d}{ds}\Big(\dot{\theta}_3 + m\rho_3 + m\rho_1\dot{\theta}_2 + m\rho_2\dot{\theta}_1 + \tfrac{h}{2}\rho_1^2\dot{\theta}_1 + h\rho_1\rho_2\Big) = -\lambda_{x3}\sin + \lambda_{y3}\cos\\
&\quad - \theta_1(\lambda_{x2}\cos + \lambda_{y2}\sin) - \theta_2(\lambda_{x1}\cos + \lambda_{y1}\sin) + \tfrac{1}{2}\theta_1^2(\lambda_{x1}\sin - \lambda_{y1}\cos). \qquad (4.25)
\end{aligned}$$

At level $l = 1, 2, 3$ the conditions (4.3) with (4.5) become

$$\rho_l\big|_0^{2\pi} = 0, \quad \dot{\rho}_l\big|_0^{2\pi} = 0, \quad \theta_l(0) = \theta_l(2\pi) = 0, \quad \dot{\theta}_l\big|_0^{2\pi} = 0. \qquad (4.26)$$

The mass constraint in (4.4) yields

$$\int_0^{2\pi} \rho_l(s)\mathrm{d}s = 0$$

whereas closedness for $l = 1, 2, 3$ results in

$$\begin{aligned}
&\int_0^{2\pi} \begin{pmatrix} -\theta_1\sin \\ \theta_1\cos \end{pmatrix} = \begin{pmatrix} 0 \\ 0 \end{pmatrix} \qquad \text{(cf. (4.13))},\\
&\int_0^{2\pi} \begin{pmatrix} -\theta_2\sin - \frac{1}{2}\theta_1^2\cos \\ \theta_2\cos - \frac{1}{2}\theta_1^2\sin \end{pmatrix} = \begin{pmatrix} 0 \\ 0 \end{pmatrix}, \qquad (4.27)\\
&\int_0^{2\pi} \begin{pmatrix} -\theta_3\sin - \theta_1\,\theta_2\cos + \frac{1}{6}\theta_1^3\sin \\ \theta_3\cos - \theta_1\,\theta_2\sin - \frac{1}{6}\theta_1^3\cos \end{pmatrix} = \begin{pmatrix} 0 \\ 0 \end{pmatrix}. \qquad (4.28)
\end{aligned}$$

4.4 Local bifurcation structure

We discuss solvability of the second- and third order perturbations of the nonlinear system (4.1)–(4.5) that we derived in Section 4.3. This allows us to characterize the local bifurcation structure of solutions in terms of the material parameters, when restricting to a quadratic bending rigidity model.

The proofs of the lemmata appearing in the remainder of this section are not detailed, they follow from tedious yet elementary computations which were verified using Mathematica.

4.4.1 Case 0: Super- and subcritical pitchfork

Recall from Proposition 4.2 that in Case 0, $\mu_0 j^2 = m^2 - \frac{h}{2}$ with $|j| \geq 2$ and $-\frac{2m^2}{j^2-1} \neq h < 2m^2 \neq 0$. The *second-order system* (4.22), (4.24), reads

$$\begin{aligned}
\mu_0\,\ddot{\rho}_2 - m\dot{\theta}_2 - \frac{h}{2}\rho_2 &= \lambda_{M2} + \frac{m}{2}\dot{\theta}_1^2 + h\rho_1\dot{\theta}_1,\\
\frac{d}{ds}\Big(\dot{\theta}_2 + m\rho_2\Big) &= -\lambda_{x2}\sin + \lambda_{y2}\cos - \frac{d}{ds}\Big(m\rho_1\dot{\theta}_1 + \frac{h}{2}\rho_1^2\Big)
\end{aligned}$$

with constraints (4.26) for $l = 2$ and (4.27). The latter reduces to θ_2 having zero first Fourier coefficients, namely

$$\int_0^{2\pi} \begin{pmatrix} -\theta_2\sin \\ \theta_2\cos \end{pmatrix} = \begin{pmatrix} 0 \\ 0 \end{pmatrix}.$$

Indeed, the first Fourier coefficients of θ_1^2 vanish because of the identities

$$\theta_1^2(s) = \left(\tfrac{a_1 m}{j}\left(\sin(js - s_1) + \sin(s_1)\right)\right)^2 = (\tfrac{a_1 m}{j})^2\left(\sin^2(js - s_1) + 2\sin(js - s_1)\sin(s_1) + \sin^2(s_1)\right),$$

$\sin^2(js - s_1) = \frac{1}{2}(1 - \cos(2(js - s_1)))$, the condition $|j| \geq 2$, and the orthogonality of trigonometric functions.

Lemma 4.4 (**Case 0: Second-order solution**). *For $a_1, a_2, s_1, s_2 \in \mathbb{R}$, $j \in \mathbb{Z}$, $|j| \geq 2$, the second-order solution reads*

$$\begin{aligned}
\rho_2(s) &= -a_2\cos(js - s_2) - \frac{a_1^2(m(m^2 - h))}{2(2m^2 - h)}\cos(2(js - s_1)),\\
\theta_2(s) &= \frac{ma_2}{j}(\sin(js - s_2) + \sin(s_2)) + \frac{a_1^2(6m^4 - 6m^2h + h^2)}{8j(2m^2 - h)}(\sin(2(js - s_1)) + \sin(2s_1)),\\
\lambda_{x2} &= \lambda_{y2} = 0, \quad \lambda_{M2} = -\frac{a_1^2(m(m^2 - 2h))}{4}.
\end{aligned}$$

The *third-order system* (4.23), (4.25) is

$$\begin{aligned}
\mu_0\,\ddot{\rho}_3 - \sigma\ddot{\rho}_1 - m\Big(\dot{\theta}_3 + \dot{\theta}_1\dot{\theta}_2\Big) - \frac{h}{2}\Big(\rho_3 + 2\rho_2\dot{\theta}_1 + 2\rho_1\dot{\theta}_2 + \rho_1\dot{\theta}_1^2\Big) &= \lambda_{M3},\\
\frac{d}{ds}\Big(\dot{\theta}_3 + m\rho_3 + m\rho_1\dot{\theta}_2 + m\rho_2\dot{\theta}_1 + \frac{h}{2}\rho_1^2\dot{\theta}_1 + h\rho_1\rho_2\Big) &= -\lambda_{x3}\sin + \lambda_{y3}\cos,
\end{aligned}$$

with constraints (4.26) for $l = 3$ and (4.28). As $\theta_1\theta_2$ and θ_1^3 both have zero first Fourier coefficients, (4.28) reduces to

$$\int_0^{2\pi}\begin{pmatrix}-\theta_3\sin\\ \theta_3\cos\end{pmatrix} = \begin{pmatrix}0\\0\end{pmatrix}.$$

Lemma 4.5 (**Case 0: Third-order solution**). *For $a_1, a_2, a_3, s_1, s_2, s_3 \in \mathbb{R}$, and $j \in \mathbb{Z}$ with $|j| \geq 2$, a solution of the third-order system exists if*

$$a_1\left(j^2\sigma - a_1^2\frac{Z(m,h)}{8(2m^2 - h)}\right) = 0 \qquad \text{with} \qquad Z(m,h) := -14m^6 + 36m^4h - 18m^2h^2 + h^3. \tag{4.29}$$

Solutions take the form

$$\begin{aligned}
\rho_3(s) &= -a_3\cos(js - s_3) - \frac{a_1a_2m(m^2 - h)}{2m^2 - h}\cos(2js - (s_1 + s_2)) - \frac{a_1^3}{4}\frac{14m^6 - 28m^4h + 14m^2h^2 - h^3}{8(2m^2 - h)^2}\cos(3(js - s_1)),\\
\theta_3(s) &= \frac{ma_3}{j}\left(\sin(js - s_3) + \sin(s_3)\right) + \frac{a_1^3m(2m^2 - 3h)}{4j}\left(\sin(js - s_1) + \sin(s_1)\right)\\
&\quad + \frac{a_1a_2(6m^2(m^2 - h) + h^2)}{4j(2m^2 - h)}\left(\sin(2js - (s_1 + s_2)) + \sin(s_1 + s_2)\right)\\
&\quad + \frac{a_1^3m(78m^6 - 156m^4h + 94m^2h^2 - 17h^3)}{96j(2m^2 - h)^2}\left(\sin(3(js - s_1)) + \sin(3s_1)\right),
\end{aligned}$$

$\lambda_{x3} = \lambda_{y3} = 0$, *and* $\lambda_{M3} = -\dfrac{a_1a_2m(m^2 - 2h)}{2}\cos(s_1 - s_2)$.

By (4.29), the amplitude of the bifurcation is thus given by

$$a_1^2 = \frac{8j^2\sigma(2m^2 - h)}{Z(m,h)} \tag{4.30}$$

and the requirement $a_1 \in \mathbb{R}$ restricts the admissible parameters m, h, and σ. In particular, as $2m^2 > h$, we have a *supercritical pitchfork bifurcation* ($\sigma = 1$) whenever $Z(m,h) > 0$. Writing $Z(m,h) = m^6(z^3 - 18z^2 + 36z - 14)$ with $z := \frac{h}{m^2} < 2$ shows that $Z(m,h) > 0$ and $2m^2 > h$ are equivalent to

$$z_1 < z < z_2 \quad \text{with} \quad z_1 \approx 0.52 \quad \text{and} \quad z_2 \approx 1.71. \tag{4.31}$$

Consequently, a supercritical pitchfork bifurcation occurs in the parabolic region $\{(m,h) \in \mathbb{R}^2 : z_1m^2 < h < z_2m^2\}$. Conversely, if (m,h) are such that $Z(m,h) < 0$, which holds for $h < z_1m^2$ or $2m^2 > h > z_2m^2$, Case 0 is a *subcritical pitchfork* ($\sigma = -1$). The situation is illustrated in Figure 4.2.

4.4.2 Case 1.0: Subcritical pitchfork

In Case 1.0, where $m = 0$, $h < 0$, and $\mu_0 = -\frac{1}{j^2}\frac{h}{2}$ for $|j| \geq 1$, the *second-order system* (4.22), (4.24) reduces to

$$\begin{aligned} \mu_0\,\ddot{\rho}_2 - \frac{h}{2}\rho_2 &= \lambda_{M2}, \\ \frac{d}{ds}\Big(\dot{\theta}_2 + \frac{h}{2}\rho_1^2\Big) &= -\lambda_{x2}\sin + \lambda_{y2}\cos \end{aligned}$$

together with the same constraints as in Case 0.

Lemma 4.6 (**Case 1.0: Second-order solution**). *For $a_1, a_2, s_1, s_2 \in \mathbb{R}$, $|j| \geq 1$, the second-order solution reads*

$$\begin{aligned} \rho_2(s) &= -a_2\cos(js - s_2), \\ \theta_2(s) &= -\frac{a_1^2 h}{8j}\Big(\sin(2(js - s_1)) + \sin(2s_1)\Big), \end{aligned}$$

and $\lambda_{x2} = \lambda_{y2} = \lambda_{M2} = 0$.

The *third-order system* (4.23), (4.25) reduces to

$$\begin{aligned} \mu_0\,\ddot{\rho}_3 - \frac{h}{2}\rho_3 &= \lambda_{M3} + \sigma\ddot{\rho}_1 + h\rho_1\dot{\theta}_2, \\ \ddot{\theta}_3 &= -\lambda_{x3}\sin + \lambda_{y3}\cos - \frac{d}{ds}\Big(h\rho_1\rho_2\Big), \end{aligned}$$

together with the same constraints as in Case 0.

Lemma 4.7 (**Case 1.0: Third-order solution**). *For $a_2, a_3, s_1, s_1, s_3 \in \mathbb{R}$, and $j \in \mathbb{Z}$ with $|j| \geq 1$, solutions of the third-order system exist if*

$$a_1\Big(j^2\sigma + \frac{a_1^2 h^2}{8}\Big) = 0 \tag{4.32}$$

and are given by

$$\begin{aligned} \rho_3(s) &= -a_3\cos(js - s_3) + \frac{a_1^3 h}{32}\cos(3(js - s_1)), \\ \theta_3(s) &= -\frac{a_1 a_2 h}{4j}\big(\sin(2js - (s_1 + s_2)) + \sin(s_1 + s_2)\big), \end{aligned}$$

and $\lambda_{x3} = \lambda_{y3} = \lambda_{M3} = 0$.

By (4.32) and $h < 0$, the bifurcation amplitude in Case 1.0 is thus given by (4.30) with $m = 0$:

$$a_1^2 = -\frac{8j^2\sigma}{h^2} = -\frac{8j^2\sigma h}{h^3} = -\frac{8j^2\sigma h}{Z(0,h)}. \tag{4.33}$$

Consequently, to obtain a nontrivial first-order solution with $a_1 \in \mathbb{R}\setminus\{0\}$, we need to assume that $\sigma = -1$. This sign amounts to perturbing the bifurcation parameter as $\mu = \mu_0 + A^2$, which shows that Case 1.0 is a *subcritical pitchfork bifurcation.*

4.4.3 Case 1.1: Subcritical bifurcation

In Case 1.1, where $h < 0$, $m \neq 0$, $\mu_0 = -\frac{h}{2} \neq \frac{m^2}{j^2-1}$ for $|j| \geq 2$, and $\theta_1 = 0$, the *second-order system* (4.22), (4.24) is

$$\begin{aligned} \mu_0\,\ddot{\rho}_2 - m\dot{\theta}_2 - \frac{h}{2}\rho_2 &= \lambda_{M2} \\ \frac{d}{ds}\Big(\dot{\theta}_2 + m\rho_2\Big) &= -\lambda_{x2}\sin + \lambda_{y2}\cos - \frac{d}{ds}\Big(\frac{h}{2}\rho_1^2\Big), \end{aligned}$$

together with the same constraints as in Case 0.

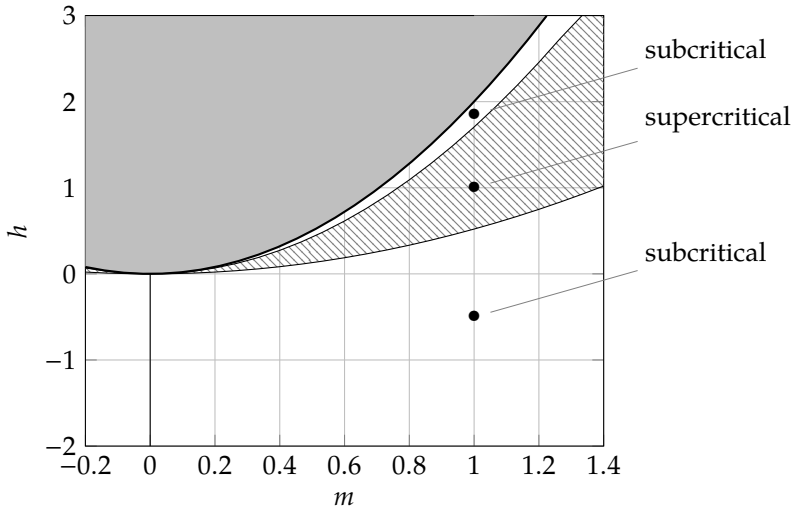

Figure 4.2: Contour plot of $Z(m,h)$ given by (4.29). The solution in Case 0 has the structure of a supercritical pitchfork bifurcation whenever $Z(m,h) > 0$ and $h < 2m^2$. These conditions define the crosshatched region $z_1 m^2 < h < z_2 m^2$ below the parabola $h = 2m^2$ (bold line); $z_1 \approx 0.52$ and $z_2 \approx 1.71$, see (4.31). Conversely, if $Z(m,h) < 0$ which is true when $h < z_1 m^2$ or in the narrow white region given by $z_2 m^2 < h < 2m^2$, then the bifurcation is subcritical.

Lemma 4.8 (**Case 1.1: Second-order solution**). *For $b_1, b_2, \tilde{s}_1, \tilde{s}_2 \in \mathbb{R}$, the second-order solution reads*

$$\rho_2(s) = -b_2\cos(s-\tilde{s}_2) - \frac{b_1^2 mh}{2(2m^2+3h)}\cos(2(s-\tilde{s}_1)),$$
$$\theta_2(s) = -\frac{3\,b_1^2h^2}{8(2m^2+3h)}\left(\sin(2(s-\tilde{s}_1)) + \sin(2\tilde{s}_1)\right),$$

and $\lambda_{x2} = -b_2 m\cos(\tilde{s}_2)$, $\lambda_{y2} = -b_2 m\sin(\tilde{s}_2)$, $\lambda_{M2} = 0$.

With $\theta_1 = 0$, the third-order system (4.23) and (4.25) reads

$$\mu_0\,\ddot{\rho}_3 - m\dot{\theta}_3 - \frac{h}{2}\rho_3 = \lambda_{M3} + \sigma\ddot{\rho}_1 + h\rho_1\dot{\theta}_2,$$
$$\frac{d}{ds}\Big(\dot{\theta}_3 + m\rho_3\Big) = -\lambda_{x3}\sin + \lambda_{y3}\cos - \theta_2\underbrace{(\lambda_{x1}\cos + \lambda_{y1}\sin)}_{=m\rho_1} - \frac{d}{ds}\Big(m\rho_1\dot{\theta}_2 + h\rho_1\rho_2\Big),$$

together with the same constraints as in Case 0.

Lemma 4.9 (**Case 1.1: Third-order solution**). *For $b_1, b_2, \tilde{s}_1, \tilde{s}_2 \in \mathbb{R}$, the third-order solution exists if*

$$b_1\Big(\sigma + b_1^2\,\frac{3h^3}{8(2m^2+3h)}\Big) = 0 \tag{4.34}$$

and is given by

$$\rho_3(s) = -b_3\cos(s-\tilde{s}_3) - \frac{b_1^3h^2}{16(2m^2+3h)}\Big(7\cos(s-\tilde{s}_1) - 6\sin(2\tilde{s}_1)\sin(s-\tilde{s}_1)\Big)$$
$$- \frac{b_1 b_2 mh}{3h+2m^2}\cos(2s-(\tilde{s}_1+\tilde{s}_2)) - \frac{3b_1^3h^2(3m^2-2h)}{16(2m^2+3h)(4h+m^2)}\cos(3(s-\tilde{s}_1)),$$
$$\theta_3(s) = -\frac{3b_1b_2h^2}{4(3h+2m^2)}\Big(\sin(2s-(\tilde{s}_1+\tilde{s}_2)) + \sin(\tilde{s}_1+\tilde{s}_2)\Big) - \frac{7b_1^3h^3m}{8(2m^2+3h)(4h+m^2)}\Big(\sin(3(s-\tilde{s}_1)) + \sin(3\tilde{s}_1)\Big),$$

and $\lambda_{x3} = -b_3 m\cos(\tilde{s}_3)$, $\lambda_{y3} = -b_3 m\sin(\tilde{s}_3)$, $\lambda_{M3} = 0$.

By (4.34),

$$b_1^2 = -\frac{8\,\sigma(2m^2+3h)}{3h^3}. \tag{4.35}$$

As Case 1 bifurcates before Case 0 whenever $h < -\frac{2}{3}m^2$, we restrict to $m^2 + \frac{3}{2}h < 0$. Consequently, as $h < 0$, we must have $\sigma = -1$ and obtain a *subcritical* bifurcation. If $-\frac{2}{3}m^2 < h < 0$ the bifurcation in Case 1.1 is *supercritical*. However, for these parameters, Case 0 occurs first.

4.5 Energy and stability

In order to discuss minimality properties and stability of the bifurcating solutions of the Euler-Lagrange equations we study the energy E_μ (1.1).

At the trivial solution $u_0 = (\rho_0, \theta_0)$ of the Euler-Lagrange equations, the first variation by definition vanishes:

$$\delta E_\mu(u_0)(\tilde{u}) := \frac{d}{dt} E_\mu(u_0 + t\tilde{u})\big|_{t=0} = 0.$$

This holds for all $\mu > 0$ and in particular at the bifurcation point $\mu = \mu_0$. The *second variation* is given by

$$\begin{aligned}
\delta^2 E_\mu(u_0)(\tilde{u}, \tilde{\tilde{u}}) &:= \frac{d^2}{dtdr} E_\mu(u_0 + t\tilde{u} + r\tilde{\tilde{u}})\big|_{t,r=0} \\
&= \int_0^L \left(\frac{\beta_0''}{2}\, \dot\theta_0^2\, \tilde{\tilde\rho}\tilde\rho + \beta_0'\, \dot\theta_0 \Big(\tilde{\tilde\rho}\dot{\tilde\theta} + \dot{\tilde{\tilde\theta}}\tilde\rho \Big) + \beta_0\, \dot{\tilde{\tilde\theta}}\dot{\tilde\theta} + \mu\, \dot{\tilde{\tilde\rho}}\dot{\tilde\rho} \right) \mathrm{d}s \\
&= \int_0^{2\pi} \left(\frac{h}{2}\, \tilde{\tilde\rho}\tilde\rho + m \left(\tilde{\tilde\rho}\dot{\tilde\theta} + \dot{\tilde{\tilde\theta}}\tilde\rho \right) + \dot{\tilde{\tilde\theta}}\dot{\tilde\theta} + \mu\, \dot{\tilde{\tilde\rho}}\dot{\tilde\rho} \right) \mathrm{d}s,
\end{aligned}$$

where in the last equality we employed the normalization (4.8) as well as $\beta_0 = 1$, $\beta_0' = m$, $\beta_0'' = h$. In particular, for $\tilde{\tilde u} = \tilde u = u_1 = (\rho_1, \theta_1)$, we get

$$\delta^2 E_\mu(u_0)(u_1, u_1) = \int_0^{2\pi} \left(\frac{h}{2}\rho_1^2 + 2m\rho_1\dot\theta_1 + \dot\theta_1^2 + \mu\dot\rho_1^2 \right) \mathrm{d}s. \tag{4.36}$$

However, it turns out that in all cases of Proposition 4.2,

$$\delta^2 E_{\mu_0}(u_0)(u_1, u_1) = 0.$$

Therefore we have to take into account higher terms in the expansion of the energy E_μ in order to decide about its minimality at (ρ_0, θ_0) and $\mu = \mu_0$. With $\mu = \mu_0 - \sigma A^2$ for $\sigma = \pm 1$, we employ the perturbation ansatz

$$(\rho, \theta) = (\rho_0, \theta_0) + A(\rho_1, \theta_1) + \sum_{l=2}^{4} A^l(\rho_l, \theta_l) + O(A^5)$$

as $A \to 0$. We need to go up to order four in order to capture effects of σ, deciding about sub- or supercriticality of the pitchfork bifurcations. In the normalized setting, the expansion reads

$$E_\mu(\rho, \theta) = \frac{1}{2} \int_0^{2\pi} (\beta(\rho)\, \dot\theta^2 + \mu\dot\rho^2)\, \mathrm{d}s = E_0 + AE_1 + A^2E_2 + A^3E_3 + A^4E_4 + O(A^5),$$

with

$$E_0 = \frac{1}{2} \int_0^{2\pi} \mathrm{d}s = \pi = E_{\mu_0}(\rho_0, \theta_0), \qquad E_1 = \frac{1}{2} \int_0^{2\pi} (m\rho_1 + 2\dot\theta_1)\, \mathrm{d}s, \tag{4.37}$$

$$E_2 = \frac{1}{2} \int_0^{2\pi} (m\rho_2 + 2\dot\theta_2 + 2m\rho_1\dot\theta_1 + \tfrac{h}{2}\rho_1^2 + \dot\theta_1^2 + \mu_0\dot\rho_1^2)\, \mathrm{d}s \tag{4.38}$$

$$\begin{aligned}
E_3 = \frac{1}{2} \int_0^{2\pi} (&m\rho_3 + 2\dot\theta_3 + 2m\rho_1\dot\theta_2 + 2m\rho_2\dot\theta_1 + m\rho_1\dot\theta_1^2 \\
&+ h\rho_1\rho_2 + h\rho_1^2\dot\theta_1 + 2\dot\theta_1\dot\theta_2 + 2\mu_0\dot\rho_1\dot\rho_2)\, \mathrm{d}s
\end{aligned} \tag{4.39}$$

$$\begin{aligned}
E_4 = \frac{1}{2} \int_0^{2\pi} (&m\rho_4 + 2\dot\theta_4 + 2m\rho_1\dot\theta_3 + 2m\rho_3\dot\theta_1 + m\rho_2\dot\theta_1^2 + 2m\rho_2\dot\theta_2 + 2m\rho_1\dot\theta_1\dot\theta_2 \\
&+ \tfrac{h}{2}\rho_2^2 + h\rho_1\rho_3 + 2h\rho_1\rho_2\dot\theta_1 + \tfrac{h}{2}\rho_1^2\dot\theta_1^2 + h\rho_1^2\dot\theta_2 + 2\dot\theta_1\dot\theta_3 + \dot\theta_2^2 + \mu_0\dot\rho_2^2 + 2\mu_0\dot\rho_1\dot\rho_3 - \sigma\dot\rho_1^2)\, \mathrm{d}s.
\end{aligned} \tag{4.40}$$

This energy expansion includes first, second, and higher variations as special cases,

$$E_1 = \delta E_{\mu_0}(\rho_0, \theta_0)(\rho_1, \theta_1), \qquad E_2\big|_{(\rho_2,\theta_2)=0} = \tfrac{1}{2}\delta^2 E_{\mu_0}(\rho_0, \theta_0)((\rho_1, \theta_1), (\rho_1, \theta_1)),$$

and similarly for higher order.

Next we insert the individual cases for (ρ_1, θ_1) according to Proposition 4.2, their higher-order perturbations, as well as the amplitudes a_1 (Case 0 and Case 1.0) or b_1 (Case 1.1).

The proofs of the following two lemmata are not detailed, they follow from tedious yet elementary computations which were verified using Mathematica.

Lemma 4.10 (**Energy expansion in Cases 0 and 1.0**). *Insertion of solutions in Case 0 and 1.0 in the energy expansion* (4.37)–(4.40) *gives* $E_1 = E_2 = E_3 = 0$ *and*

$$E_4 = -\frac{2\pi j^4(2m^2 - h)}{Z(m,h)} \tag{4.41}$$

for $j \in \mathbb{Z}$ *with* $|j| \geq 2$ *and with* $Z(m,h) = h^3 - 18m^2h^2 + 36m^4h - 14m^6$ *from Lemma 4.5. For* $m = 0$ *this reduces to Case 1.0, where* $Z(0,h) = h^3$ *as in Lemma 4.7,* $|j| \geq 1$*, and*

$$E_4 = \frac{2\pi j^4}{h^2}.$$

Lemma 4.11 (**Energy expansion in Case 1.1**). *Insertion of solutions in Case 1.1 in the energy expansion* (4.37)–(4.40) *gives* $E_1 = E_2 = E_3 = 0$ *and*

$$E_4 = \frac{2\pi(3h + 2m^2)}{3h^3}. \tag{4.42}$$

The energy expansion of Lemma 4.10 and Lemma 4.11 allows us to determine the *stability* of solution branches: As with $A \to 0$,

$$E_\mu(\rho,\theta) = E_{\mu_0}(\rho_0,\theta_0) + A^4E_4 + O(A^5),$$

the sign of the fourth-order energy is decisive. If $E_4 > 0$ then the trivial branch (ρ_0,θ_0) is stable at the bifurcation point μ_0, whereas it will lose its stability if $E_4 < 0$. As by assumption $h < 2m^2$ in Case 0, the sign of E_4 is determined by that of $Z(m,h)$. Therefore the stability behavior is in consistence with the sup- or supercriticality of solutions. In Case 1.0 we always have $E_4 > 0$ (unstable bifurcation), which is consistent with the subcriticality of the bifurcation. Finally, Case 1.1 is subcritical for $3h + 2m^2 < 0$, which gives instability ($E_4 > 0$). Conversely, we have stability ($E_4 > 0$) whenever $-\frac{3}{2}m^2 < h < 0$, which is the supercritical situation for Case 1.1.

5 Numerical continuation of bifurcation branches

5.1 Discretization

The Euler-Lagrange equations (4.1) and (4.2) are discretized by finite differences as follows. For $N \in \mathbb{N}$ we discretize the interval $[0,L]$ by introducing $\Delta s = L(N-1)^{-1}$ and $s_i = i\Delta s$, $0 \leq i \leq N-1$, which naturally leads to the (abuse of) notation $\rho = (\rho_i)_{i=1}^{N-1}$, $\theta = (\theta_i)_{i=1}^{N-1}$ with $\rho_i = \rho(s_i)$, $\theta_i = \theta(s_i)$. This can be thought of as considering a polygonal approximation of the curve γ, where θ_i is the angle of the i^{th} side and where ρ_i is a piecewise constant approximation of ρ on that side (*i.e.* ρ_i is *not* associated to a vertex).

Using the notation $u = (\rho,\theta)$ and $\Lambda = (\lambda_M, \lambda_x, \lambda_y)$, we propose the following natural finite differences approximation for (4.1) and (4.2), respectively:

$$EL_\rho(u,\Lambda) = \mu\left(\frac{\rho_{i-1} - 2\rho_i + \rho_{i+1}}{\Delta s^2}\right) - \frac{1}{2}\beta'(\rho_i)\left(\frac{\rho_{i+1} - \rho_{i-1}}{2\Delta s}\right)^2 - \lambda_M = 0\,, \tag{5.1}$$

$$EL_\theta(u,\Lambda) = \frac{1}{\Delta s}\left(\beta\left(\frac{\rho_{i+1} + \rho_i}{2}\right)\left(\frac{\theta_{i+1} - \theta_i}{\Delta s}\right) - \beta\left(\frac{\rho_i + \rho_{i-1}}{2}\right)\left(\frac{\theta_i - \theta_{i-1}}{\Delta s}\right)\right) + \lambda_x\sin\theta_i - \lambda_y\cos\theta_i = 0\,, \tag{5.2}$$

for $0 \leq i \leq N-1$.

To remove the degree of freedom associated to solid rotations, we can set $\theta(0) = 0$ at the continuous level. This is reflected by the choice $\theta_0 = 0$ at the discrete level. We also need to provide values for indices $i = -1, N$. Again by periodicity we set $\rho_{-1} = \rho_{N-1}$, $\rho_N = \rho_0$, $\theta_{-1} = \theta_{N-1} - 2\pi$, and $\theta_N = \theta_0 + 2\pi$. Thus, we only consider (5.1) for $0 \leq i < N-1$ and (5.2) for $0 < i < N-1$.

The mass and closedness constraints can be naturally approximated as

$$C_M(u,\Lambda) = \Delta s\sum_{i=0}^{N-1}\rho_i - M = 0\,,$$

$$\begin{pmatrix} C_x \\ C_y \end{pmatrix}(u,\Lambda) = \Delta s\sum_{i=0}^{N-1}\begin{pmatrix}\cos\theta_i \\ \sin\theta_i\end{pmatrix} = 0\,.$$

We are left with a system of $2N+1$ non linear equations which we propose to solve using a damped Newton method. If we assume $\bar{u}^k = \left(u^k, \Lambda^k\right)$ to be known, we look for $\bar{u}^{k+1}$ as a solution to

$$J(\bar{u}^k)\,(\bar{u}^{k+1} - \bar{u}^k) = -\eta\, r(\bar{u}^k)\,, \tag{5.3}$$

where $r(\bar{u}^k) = (EL_\rho, EL_\theta, C_M, C_x, C_y)$, J is the Jacobian of r with respect to $\bar{u}$, and $\eta \leq 1$ is the damping parameter with $\eta = 1$ corresponding to the standard Newton's method.

5.1.1 Continuation of branches

To follow numerically the bifurcation branches, one can pick some μ close to the critical value μ_0 and take as initial value a perturbation of the trivial solution (corresponding to the circle with homogeneous ρ, see Proposition 4.1). The position of μ relative to the critical value and the amplitude of the bifurcation are given precisely by the results of Section 4.4. Solving (5.3) yields a numerical approximation of a critical point, which can be used as initial condition for neighbouring values of μ. By iterating this process, one can move along the branch, provided that

1. the branch is locally smooth (for example, this is not the case when ρ hits zeros of β, where one could expect the branch to terminate),
2. the features of the solution can be resolved by the discretization with the chosen value of N.

5.2 Choice of parameters

In the what follows we will consider a number of different situations, depending on the choice of parameters (m, h) for the function β, which will be of the form (4.6) with $\beta_0 = 1$, namely

$$\beta(\rho) = 1 + m\,(\rho - \rho_0) + \frac{h}{2}\,(\rho - \rho_0)^2\,.$$

We will take $M = L = 2\pi$, so that $\rho_0 = 1$ and consider six sets of parameters:

(i) $(m, h) = (1, 1.85)$ corresponding to Case 0 with $\sigma = -1$ (subcritical bifurcation),

(ii) $(m, h) = (1, 1)$ corresponding to Case 0 with $\sigma = 1$ (supercritical bifurcation),

(iii) $(m, h) = (1, 1/4)$ corresponding to Case 0 with $\sigma = -1$ (subcritical bifurcation),

(iv) $(m, h) = (1, -1/2)$ corresponding to Case 0 with $\sigma = -1$ (subcritical bifurcation) and supercritical Case 1.1,

(v) $(m, h) = (1, -2)$ corresponding to Case 0 with $\sigma = -1$ (subcritical bifurcation) and subcritical Case 1.1,

(vi) and $(m, h) = (0, -1)$, which corresponds to Case 1.0, where we expect a subcritical bifurcation and that at first order, γ remains a circle. We also expect a branch of critical points corresponding to $j = 1$, contrary to the other two cases.

For the definition of the different cases, we refer to Proposition 4.2. The parameters in (i) – (vi) are represented on Figure 5.1. The corresponding results are presented in Figures 5.3 and 5.4.

5.3 Results

The method described above (Section 5.1) was implemented in `Julia` [3]. Figure 5.3 presents the bifurcating branches both in terms of the amplitude of the density ρ and in terms of the energy E_μ. It offers a partial confirmation of the results of Section 4.4 in that:

- For Case (ii), $j \geq 2$ and (iv), $j = 1$, the bifurcation appears supercritical, *i.e.* the branch bifurcates to the left of the critical μ. Additionally, the energy decreases close to the trivial state. These branches offer critical points of E_μ which are candidates to be global minimizers.
- For all other cases, the bifurcation is subcritical, *i.e* the branch bifurcates to the right of the critical μ, and the energy initially increases as one gets further from the trivial state.

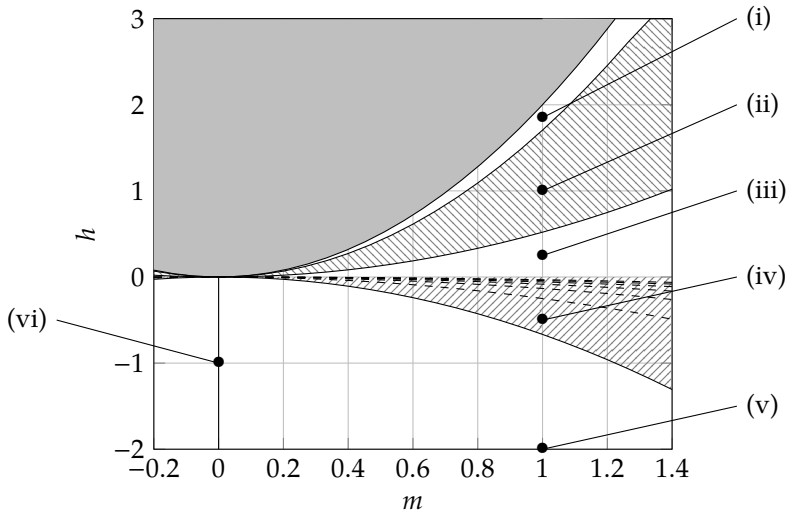

Figure 5.1: The different sets of model parameters (m, h) represented on the parameter space. The gray region corresponds to parameters which have no critical points except the trivial solution. The crosshatched region corresponds to supercritical bifurcations (Case 0 for $h > 0$, Case 1.1 for $h < 0$), and the plain white region to subcritical bifurcations. The dashed parabolas indicate where Case 2 occurs, for j up to 8.

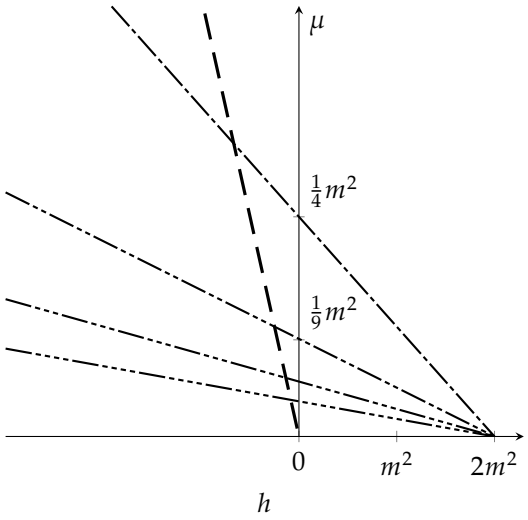

Figure 5.2: Critical values of μ for Case 0 (thin) and Case 1 (bold). The intersections correspond to (the degenerate) Case 2 which is not studied in this paper. The dashes indicate the value of j: — — for $j = 1$, — - — for $j = 2$, etc.

Interestingly, Cases (i) and (iv) feature turning points, where the derivative of E_μ along the branch seems to change sign. In Case (i) it becomes negative, leading to critical points of lower energy w.r.t. the trivial state, and potentially global minimizers.

We were able to track an additional branch in Cases (i) to (iii), which seem to bifurcate from the $j = 2$ branch. No analytical results are available at this point, but we can make the following observations. The corresponding shapes, presented in gray in Figure 5.4, look like the ones obtained for $j = 1$ in Cases (iv) to (vi). This justifies the placement in the first column, although j has no meaning for this branch. In Cases (i) and (iii), it bifurcates from the $j = 2$ branch with decreasing energy for the choice of parameter considered. Case (ii) is a bit different, in that the bifurcation leads to critical points of higher energy, although the branch features a turning point, after which E_μ starts decreasing and eventually becomes smaller than for the $j = 2$ branch, for a given value of μ.

Other features of the critical points further along the branch can be seen in Figure 5.4, where one can clearly identify the value of $j = 2$ with the number of flatter sections in each closed curve (with perhaps the exception of Case (iv) for $j = 1$). These correspond to higher values of ρ, which agree with the fact that for all choices of

parameters presented here, $m \geq 0$. This can be roughly thought as higher values of ρ penalizing higher values of the curvature $\dot{\theta}$.

Additionally, *far* from the bifurcation point and after potential turning points, one can distinguish Cases (i) and (ii) from Cases (iii) to (vi). For the former, μ decreases along the branch, E_μ decreases and ρ seems to concentrate on flat sections. For the latter, the situation is the opposite: μ increases along the branch, E_μ increases and ρ stays rather smooth.

Remark 5.1. In Proposition 3.3 it is stated that for β bounded away from 0, only the trivial state (ρ_0, θ_0) is a minimizer of E_μ. The branches in Figure 5.3 which seem to continue far to large values of μ have an energy clearly larger than $\pi = E_\mu(\rho_0, \theta_0)$. We also recall that for the results presented here, the choice of β is quadratic, and thus not bounded away from 0. There is then no contradiction of our analysis.

A systematic study of the stability in terms of the energy would be interesting, although probably necessarily limited to numerics, as it would help identifying local minimizers. Such an investigation is however out of the scope of this paper.

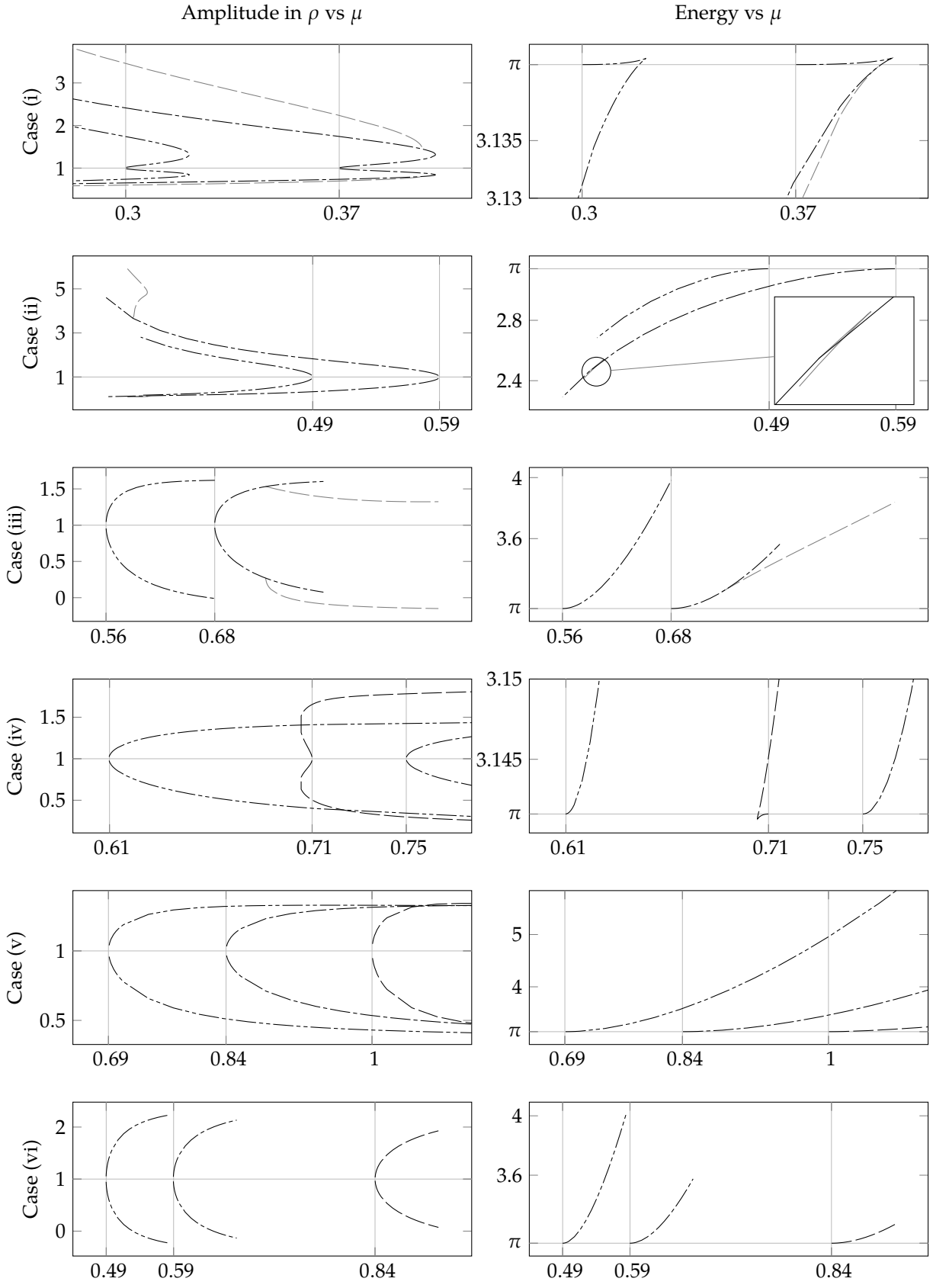

Figure 5.3: Numerical results for Cases (i) to (vi), in columns, for $j \leq 2$. The first column shows the amplitude in ρ, where the lower and greatest values of ρ are represented. The horizontal gray line corresponds to the trivial solution, for which $\rho \equiv 1$. The second column shows the energy E_μ, with the horizontal gray line again corresponding to the trivial solution, for which $E_\mu = \pi$. The dashes indicate the value of j for each branch: — — for $j = 1$ (absent in (i) to (iii)), — - — for $j = 2$, — - - — for $j = 3$. The gray vertical lines indicate the theoretical critical values for μ. In Cases (i) to (iii), the secondary bifurcation branch is plotted in gray. As detailed in (4.21), at a supercritical (resp. subcritical) bifurcation point, the branch will appear for values of μ greater (resp. lower) than the critical value.

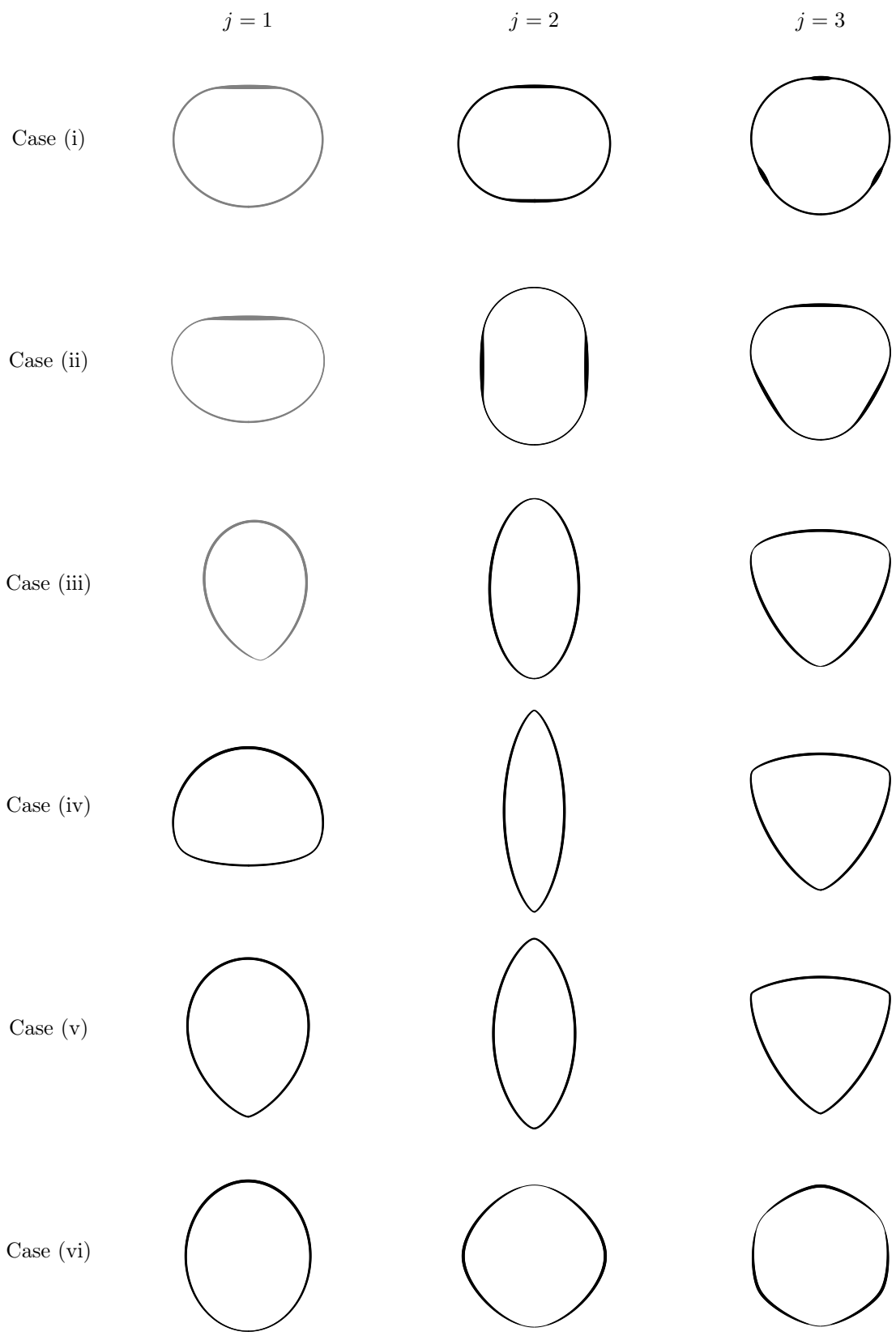

Figure 5.4: The shapes corresponding to each case, with $j = 1, 2, 3$ increasing with each column. These correspond to the last point computed on the branches shown in Figure 5.3. In Cases (i) to (iii), the shapes in the first column are in gray, as they do not correspond to branches bifurcating from the trivial state, and j is not defined in this case. They are placed in the first column due to their resemblance to shapes obtained for $h < 0$, in Cases (iv) to (vi). Thicker lines denote larger values of ρ. In Cases (i) to (v) we have $m > 0$ and β is increasing locally around the trivial solution: regions of high curvature "avoid" high values of ρ. In Case (vi) β is flat and symmetrical around ρ_0, so that the numbers of corners is twice the value of j and is always even. At the corners, ρ alternates between its extrema and varies smoothly in between.

Acknowledgements

This work has been supported by the Austrian Science Fund (FWF) projects F 65, W 1245, P 32788, by the Vienna Science and Technology Fund (WWTF) through Project MA14-009, and by the Austrian Academy of Sciences via the New Frontier's grant NST 0001.

References

[1] J. M. Ball and R. D. James. Fine phase mixtures as minimizers of energy. *Archive for Rational Mechanics and Analysis*, 100(1):13–52, 1987.

[2] T. Baumgart, S. T. Hess, and W. W. Webb. Imaging coexisting fluid domains in biomembrane models coupling curvature and line tension. *Nature*, 425(6960):821–824, Oct. 2003.

[3] J. Bezanson, A. Edelman, S. Karpinski, and V. B. Shah. Julia: a fresh approach to numerical computing. *SIAM Review*, 59(1):65–98, 2017.

[4] K. Brazda, L. Lussardi, and U. Stefanelli. Existence of varifold minimizers for the multiphase Canham-Helfrich functional. *Calculus of Variations and Partial Differential Equations*, 59(3):Paper No. 93, 26, 2020.

[5] P. B. Canham. The minimum energy of bending as a possible explanation of the biconcave shape of the human red blood cell. *Journal of Theoretical Biology*, 26(1):61 – 81, 1970.

[6] R. Choksi, M. Morandotti, and M. Veneroni. Global minimizers for axisymmetric multiphase membranes. *ESAIM. Control, Optimisation and Calculus of Variations*, 19(4):1014–1029, 2013.

[7] M. G. Crandall and P. H. Rabinowitz. Bifurcation from simple eigenvalues. *J. Functional Analysis*, 8:321–340, 1971.

[8] B. E. J. Dahlberg. The converse of the four vertex theorem. *Proceedings of the American Mathematical Society*, 133(7):2131–2135, 2005.

[9] M. P. do Carmo. *Differential geometry of curves and surfaces*. Prentice-Hall, Inc., Englewood Cliffs, N.J., 1976.

[10] W. Helfrich. Elastic Properties of Lipid Bilayers: Theory and Possible Experiments. *Zeitschrift für Naturforschung C*, 28(11-12):693–703, Dec. 1973.

[11] M. Helmers. Snapping elastic curves as a one-dimensional analogue of two-component lipid bilayers. *Mathematical Models and Methods in Applied Sciences*, 21(5):1027–1042, 2011.

[12] M. Helmers. Convergence of an approximation for rotationally symmetric two-phase lipid bilayer membranes. *The Quarterly Journal of Mathematics*, 66(1):143–170, 2015.

[13] J. Langer and D. A. Singer. Curve straightening and a minimax argument for closed elastic curves. *Topology. An International Journal of Mathematics*, 24(1):75–88, 1985.

[14] J. E. Marsden and T. J. R. Hughes. *Mathematical foundations of elasticity*. Dover Publications, Inc., New York, 1994.

[15] H. T. McMahon and J. L. Gallop. Membrane curvature and mechanisms of dynamic cell membrane remodelling. *Nature*, 438(7068):590–596, Dec. 2005.

[16] B. Palmer and Á. Pámpano. Anisotropic bending energies of curves. *Annals of Global Analysis and Geometry*, 57(2):257–287, 2020.

[17] C. Truesdell. The influence of elasticity on analysis: the classic heritage. *Bull. Amer. Math. Soc. (N.S.)*, 9(3):293–310, 1983.